DOI: 10.1002/chem.200702002

Reactivity of Silole within a Core-Modified Porphyrin Environment: Synthesis of 21-Silaphlorin and its Conversion to Carbacorrole

Janusz Skonieczny, Lechosław Latos-Grażyński,* and Ludmiła Szterenberg[a]

Abstract: Condensation of 1,1-dimethyl-3,4-diphenyl-2,5-bis(*p*-tolylhydroxymethyl)silole with pyrrole and *p*-tolylaldehyde did not form the expected 21,21-dimethyl-2,3-diphenyl-5,10,15,20-tetra(*p*-tolyl)-21-silaporphyrin, but rather its reduced derivative, 21-silaphlorin, which contains a tetrahedrally hybridised C5 carbon atom. Attempts to trap 21-silaporphyrin resulted in the serendipitous discovery of a unique transformation of 21-silaphlorin into a non-aromatic isomer of 2,3-diphenyl-5,10,15,21-tetra(*p*-tolyl)-carbacorrole (*iso*-carbacorrole). This novel carbaporphyrinoid contains a cyclopentadiene ring embedded in a tripyrrolic framework. This transformation of 21-silaphlorin to *iso*-carbacorrole, carried out under oxidative conditions, involves extrusion of dimethylsilylene accompanied by migration of the C_{meso}-(*p*-tolyl) unit to create a cyclopentadiene ring directly linked to the adjacent pyrrole through a tetrahedral carbon atom. Insertion of silver or copper ions into *iso*-carbacorrole gave two structurally related organometallic complexes of "true" carbacorrole in which the metal(III) ions are bound by three pyrrolic nitrogen atoms and a tetrahedrally hybridised C21 atom of the cyclopentadiene moiety. In the presence of oxygen, the silver(III) carbacorrole undergoes internal oxidation to 21-oxacorrole. The structure of silver(III) carbacorrole was determined by X-ray crystallography. The C21 atom was found to have a tetrahedral geometry. The Ag–C(sp^3) (2.046(5) Å) bond length is similar to that in silver(III) carbaporphyrinoids in which a trigonal carbon atom coordinates to the metal ion. Density functional theory was applied to model the molecular and electronic structure of 21-silaphlorin and feasible isomers of carbacorrole. The total energies (kcal mol^{-1} vs. *iso*-carbacorrole), calculated at the B3LYP/6-31G**//B3LYP/6-31G* level for carbacorrole, *iso*-carbacorrole, vacataporphyrin and cyclobutadienephlorin, demonstrate the energetic preference for *iso*-carbacorrole.

Keywords: corroles · heteroporphyrins · porphyrinoids · rearrangement · siloles

Introduction

Porphyrinoids, including carbaporphyrinoids, can be derived from regular porphyrins by means of contraction, isomerisation, expansion or core modification concepts.[1–4]

Thus heteroporphyrins **1**-X are formally related to regular porphyrins by replacement of an NH fragment by a heteroatom (X), typically from Group 16 of the periodic table. An analogous group of modifications involves the introduction of a C–H moiety into the porphyrin core to afford carbaporphyrinoids.

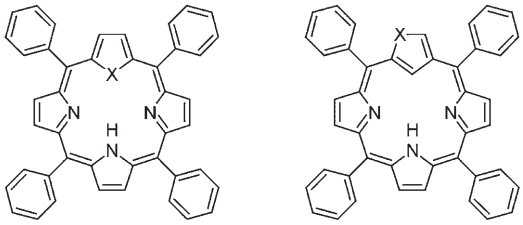

1-X X = O, S, Se, Te, PR, SiR_2 **2**-X X = O, S, NH

In the macrocyclic environment, a heteroatom can function as a donor toward a variety of metal ions, and offers an insight into the coordination properties of furan, thiophene or selenophene.[5–7] The metal–heteroatom bond is firmly held in the cavity of heteroporphyrin and dissociation of the M–X bond is generally not observed. A peculiar alteration of the reactivity of heterocyclopentadiene within a core-

[a] J. Skonieczny, Prof. Dr. L. Latos-Grażyński, Dr. L. Szterenberg
Department of Chemistry, University of Wrocław
14 F. Joliot-Curie St., Wrocław 50 383 (Poland)
Fax:(+48) 71-328-2348
E-mail: LLG@wchuwr.chem.uni.wroc.pl

Supporting information for this article is available on the WWW under http://www.chemeurj.org/ or from the author.

modified porphyrin environment was observed. For instance, 21-telluraporphyrin **1**-Te is converted by oxidation with peroxybenzoic acid into the 21-oxaporphyrin (**1**-O).[8] The reaction of **1**-Te with 1 M aqueous HCl gave 21,21-dichloro-21-telluraporphyrin.[9] Substraction of a tellurium atom from **1**-Te yielded aza-deficient porphyrin 5,10,15,20-tetraaryl-21-vacataporphyrin.[10]

Considering the peculiar structural properties, it is significant to recall that 21,23-ditelluraporphyrin is the first analogue of [18]porphyrin(1.1.1.1) with a non-planar macrocyclic conformation containing a flipped five-membered ring.[11]

In constructing a non-trivial macrocyclic environment for organometallic chemistry, the heteroatom confusion (X-confusion) concept, originally exemplified by a porphyrin–2-aza-21-carbaporphyrin couple,[12,13] was applied.[3,4] Consequently, interchanging the heteroatom with a β-methine group transforms the regular heteroporphyrin **1**-X into the X-confused isomer **2**-X. This strategy resulted in formation of thia and oxa analogues of *N*-confused porphyrin in which the sulfur or oxygen is located on the periphery of the macrocycle.[14–19] Finally, interchanging a nitrogen atom with a β-methine group transforms the regular heteroporphyrin into the *N*-confused isomer.[20,21]

In general, a reaction between 2,5-bis(arylhydroxymethyl)heterocyclopentadiene and pyrroles produced a variety of 5,10,15,20-tetraphenyl-21,23-diheteroporphyrins.[5,22–26] Once arylaldehyde was included in the condensation, 5,10,15,20-tetraaryl-21-heteroporphyrins were produced as well.[5,6,8,26–28] In the course of a typical synthesis in analogy to the formation of *N*-confused tetraarylporphyrin,[12,13] *N*-confused heteroporphyrins were accompanied by formation of heteroporphyrins.[20,21] The use of X-confused derivatives 2,4-bis(arylhydroxymethyl)heterocyclopentadiene instead of a regular counterpart afforded X-confused heteroporphyrins.[15,17,19] The recent seminal reports by Matano and coworkers on the synthesis of 21-phospha-23-thiaporphyrin,[29] phosphole-containing calixpyrroles[30] and calixpyrins[31] presented the replacement of nitrogen by phosphorous for the very first time. This remarkable step in the field of core-modified porphyrins provides an incentive to search for porphyrinoids that contain a built-in non-trivial heteroatom.

Herein, we report the synthesis and characterisation of 21-silaphlorin and its conversion into *iso*-carbacorrole. This unique reaction demonstrates the remarkable ability of the macrocyclic environment to influence the fundamental reactivity of the silole moiety.

Results and Discussion

Synthesis of 2,5-bis(arylhydroxymethyl)-1,1-dimethylsilole: A key step in the synthesis of 5,10,15,20-tetrarylsilaporphyrinoids is the construction of 2,5-bis(arylhydroxymethyl)-1,1-dimethylsilole, which is a suitable synthon for introducing the silole ring into a porphyrin-like skeleton. We used the one-pot silole cyclisation method of Tamao (Scheme 1).[32–34]

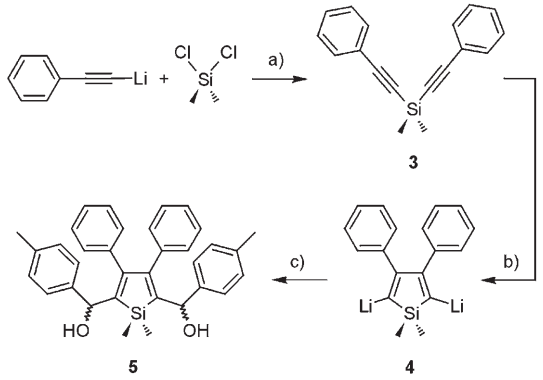

Scheme 1. Synthesis of 1,1-dimethyl-3,4-diphenyl-2,5-bis(*p*-tolylhydroxymethyl)silole (**5**): a) 0.05 equiv CuCN, THF, 0 °C, N_2, 3 h; b) 4 equiv LiNaph, THF, room temperature, N_2, 1 h; c) 4 equiv *p*-tolylaldehyde, THF, −78 °C, 1 h, N_2.

The intramolecular reductive cyclisation of bis(phenylethynyl)dimethylsilane (**3**) with excess lithium naphthalenide yielded quantitatively 2,5-dilithiosilole **4**. Subsequently, four equivalents of *p*-tolylaldehyde were added to the mixture to give 1,1-dimethyl-3,4-diphenyl-2,5-bis(*p*-tolylhydroxymethyl)silole (**5**). Excess *p*-tolylaldehyde quenched an excess of lithium naphthalenide. Chromatography and recrystallisation from toluene separated the racemate (**5**-*SS* and **5**-*RR*) and *meso*-form (**5**-*RS*) of **5**. The diastereomers are easily identified by NMR spectroscopy because of the apparent difference in the molecular symmetry (**5**-*SS*, C_2; **5**-*RS*, C_s).

Accordingly, a single silicon-bound methyl resonance ($\delta =$ −0.13 ppm), but two (0.5 and −0.85 ppm) were detected for **5**-*SS* (*RR*) and **5**-*RS*, respectively. The ^{1}H,^{29}Si scalar coupling detected by an HMBC experiment confirmed the assignments. The impressive chemical shift difference reflects the mutual orientation of the Si-methyl and *p*-tolyl groups, as shown in Figure 1. In the extreme case of **5**-*RS*, the upfield-shifted resonance corresponds to the methyl located in the

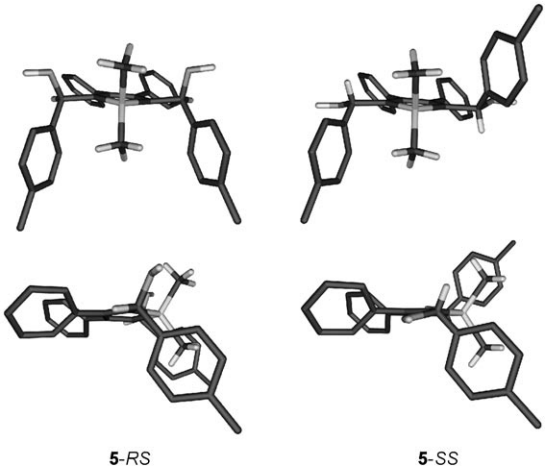

Figure 1. Drawing of the **5**-*RS* and **5**-*SS* structures (top: front projections, bottom: side projections) as obtained from the molecular mechanics calculations.

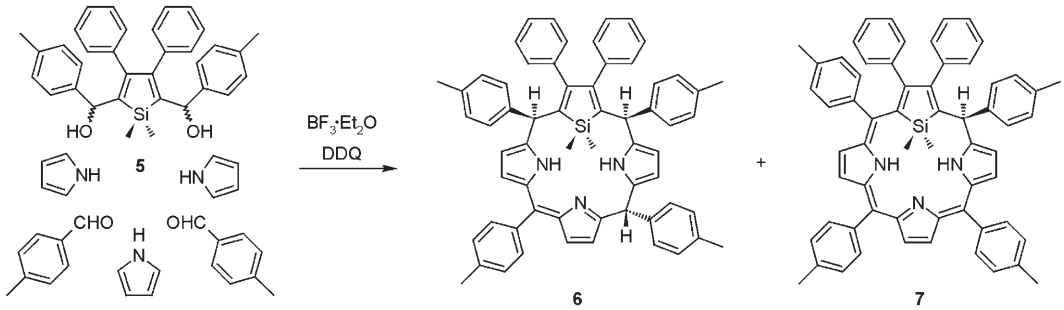

Scheme 2. Synthesis of 21-silaporphyrinoids.

shielding zone of two adjacent aryls whereas its counterpart positioned on the other side of the silole ring stays away from this influence. Accordingly, the **5**-*SS* (*RR*) spectrum reveals shielding by a single *meso*-aryl to give an intermediary chemical shift.

Synthesis and characterisation of 21-silaporphyrinoids: The synthetic work leading to 21-silaporphyrinoids is summarised in Scheme 2.

The synthesis involves the one-pot reaction of 1,1-dimethyl-3,4-diphenyl-2,5-bis(*p*-tolylhydroxymethyl)silole (**5**) with pyrrole and *p*-tolylaldehyde (1:3:2 molar ratio), carried out in dichloromethane, catalysed by $BF_3{\cdot}Et_2O$, followed by oxidation with 2,3-dichloro-5,6-dicyano-1,4-benzoquinone (DDQ). The procedure follows the methodology previously utilised for the synthesis of heteroporphyrins or carbaporphyrinoids[5] and the intended product was 21-silaporphyrin (**1**-$SiMe_2$). Instead of the expected 21-silaporphyrin, two macrocyclic products were isolated after chromatographic workup: dihydro-21-silaphlorin **6** and 21-silaphlorin **7**, albeit in rather minute yields. In some experiments, *iso*-carbacorrole (*iso*-**8**, Scheme 3) was detected as well, which was even-

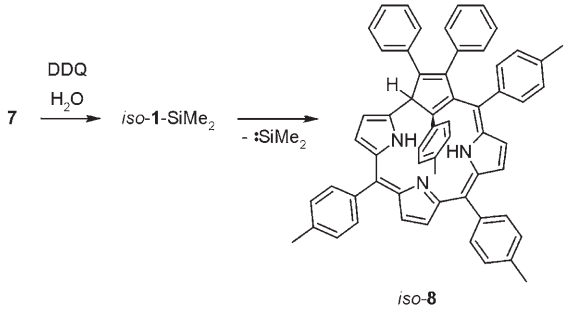

Scheme 3. Formation of *iso*-**8**.

tually attributed to the presence of traces of water in the oxidation step (see below).

Clearly, further oxidation of markedly puckered **7** to produce **1**-$SiMe_2$ (or its isomer *iso*-**1**-$SiMe_2$) is hindered and accompanied by rather unexpected processes (see below). The steric barrier is primarily imposed by the dimethyl substitution of the Si21 atom. Because a single methyl group can

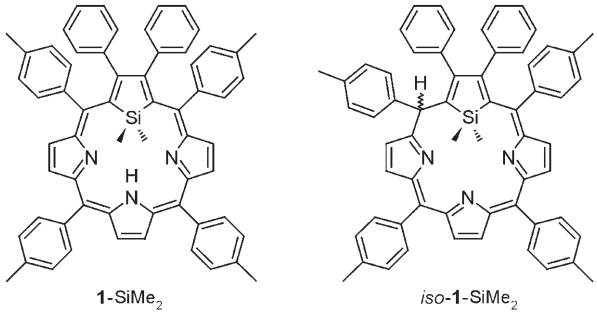

not be threaded through the porphyrin centre, the silole ring must remain tilted with respect to the tripyrrolic plane at each oxidation state and thus obstructs planarisation and consequently aromatisation. The preference for 21-silaphlorin formation remained in contrast with the reported chemistry of phlorins. Thus phlorins are reduced porphyrin derivatives that contain four pyrroles bridged by three sp^2 and one sp^3 *meso*-carbon atoms. They are readily converted into more stable porphyrins via oxidation and consequently they are typically not detectable in regular porphyrin syntheses. Usually only a controlled reduction of porphyrins or *N*-substituted porphyrins afforded stable phlorins.[16,35–42]

Formation of *iso*-carbacorrole: Several attempts were made to force further oxidation of **6** and **7** with the ultimate aim of trapping **1**-$SiMe_2$. Adjustments of the reaction conditions involved changing the amount of DDQ, increasing the reaction temperature or the use of other oxidising reagents. Oxidation was followed systematically by mass spectrometry and ^1H NMR spectroscopy. Thus an addition of a stoichiometric amount of DDQ to the sample of **7** in [D]chloroform resulted in severe broadening of all ^1H NMR resonances, which suggests merely the formation of a radical species that, even if present in a minute amount, may lead to significant line broadening.[43–46]

The ESI spectrum measured immediately after addition of DDQ to the solution of the sample in chloroform yielded an intense peak at $m/z = 866.4$, which corresponds to the molecular formula of **1**-$SiMe_2$ or its isomer *iso*-**1**-$SiMe_2$. Separate peaks in the same spectrum were readily assigned to oxygen or dioxygen adducts of **1**-$SiMe_2$ or to its desilylation products. The composition of the reaction mixture was sys-

tematically probed by ESI and revealed that the **1**-$SiMe_2$ species is unstable. On standing at 298 K for 1 minute, the peaks attributed to the starting species decrease in intensity and eventually completely decay after 15 minutes.

Our efforts to trap 21-silaporphyrin (**1**-$SiMe_2$) eventually resulted in the serendipitous discovery of a unique inner macrocyclic transformation: under oxidative conditions, 21-silaphlorin **7** converts into a non-aromatic isomer of carbacorrole, namely *iso*-carbacorrole (*iso*-**8**, Scheme 3) the structure of which resembles the recently reported *P*-confused-phosphacorrole.[47] Typically, *iso*-**8** can be obtained by condensation of **5**, pyrrole and arylaldehyde, as described in the Experimental Section. Significantly for mechanistic considerations, the combined NMR and MS investigations revealed that 21-silaphlorin **7** transforms into *iso*-**8** after addition of DDQ. In general, carbacorrole is a novel carbaporphyrinoid with a cyclopentadiene ring embedded in the tripyrrolic framework. Previously, the synthesis of the corrole isomer that is, *N*-confused corrole which is formally constructed by interchanging a pyrrolic N22 nitrogen atom with a β-methine C7, was briefly reported[48] providing the first example of an aromatic carbaporphyrinoid confined in a corrole frame.

This process was eventually attributed to the extrusion of silylene (:$SiMe_2$) from the 21-silaphlorin skeleton (Scheme 4) and ring contraction of the 21-silaporphyrin to *iso*-carbacorrole. This remarkable rearrangement has an analogy in regular porphyrin chemistry reported by Callot and co-workers.[49–51] Namely, the acylation of nickel(II) *meso*-tetraarylporphyrins resulted in ring contraction of the regular porphyrin to a corrole, explained by pinacolic rearrangement reminiscent of the one taking place during formation of corrinoids. Presumably the transformation requires the initial oxidation of 21-silaphlorin to be accompanied by a reaction centred at the silicon atom with water. The formal oxidation state of the macrocycle **8** remains unchanged in comparison to parent **7**. The isomerisation of **8** into *iso*-**8** resembles the tautomerism detected for 6-amino-fulvene-aldimines. In this group of compounds, the process involves migration of a hydrogen around a cyclopentadiene ring.[52]

2,5-Diphenylsiloles have been known to be desilylated under basic conditions to produce the corresponding butadiene derivatives.[53–56] We initially considered the formation of cyclobutadienephlorin **11** (see below) and assumed that the macrocyclic constraints force the cyclobutadiene ring to close instead of the acyclic butadiene structure. Facile silylene extrusion was previously reported from 1,1-diarylsilacyclopropenes to afford the corresponding alkynes (thermal conditions)[57,58] and from 1,1-diamino-2,3-bis(trimethylsilyl)-silacyclopropene (photochemical conditions).[59,60] Several methods can be applied to generate cyclobutadiene, as illustrated by the selected examples which involve an extrusion step from a preformed heterocyclopentadiene derivative.[61–64]

NMR investigations: The identities of **6**, **7** and *iso*-**8** were confirmed by high-resolution mass spectrometry and NMR spectroscopy. The assignments of the 21-silaphlorin resonances, which are given above selected groups of peaks in Figure 2, were made on the basis of relative intensities and detailed two-dimensional NMR studies (COSY, NOESY, ^1H,^{13}C (HMQC, HMBC) and ^1H,^{29}Si (HMBC)) carried out at 230 K in [D_2]dichloromethane.

The ^1H NMR spectrum of **7** (230 K) exhibits three AB patterns. Four different sets of *meso*-*p*-tolyl ring resonances were detected. Two of them demonstrated two *ortho* and two *meta* multiplets that were readily correlated with particular methyl resonances by COSY and NOESY. The detected differentiation of *ortho* and *meta* resonances seen for 10,15-*p*-tolyls suggests that their rotation with respect to the C_{meso}–C_{ipso} bond is slow below 230 K and obviously the macrocycle is not planar. In contrast, fast rotation was detected for 5- and 20-*p*-tolyls that are adjacent to the silole moiety, as documented by a single doublet for the *ortho* and *meta* positions in each case. Indeed, the phenyl rings attached at

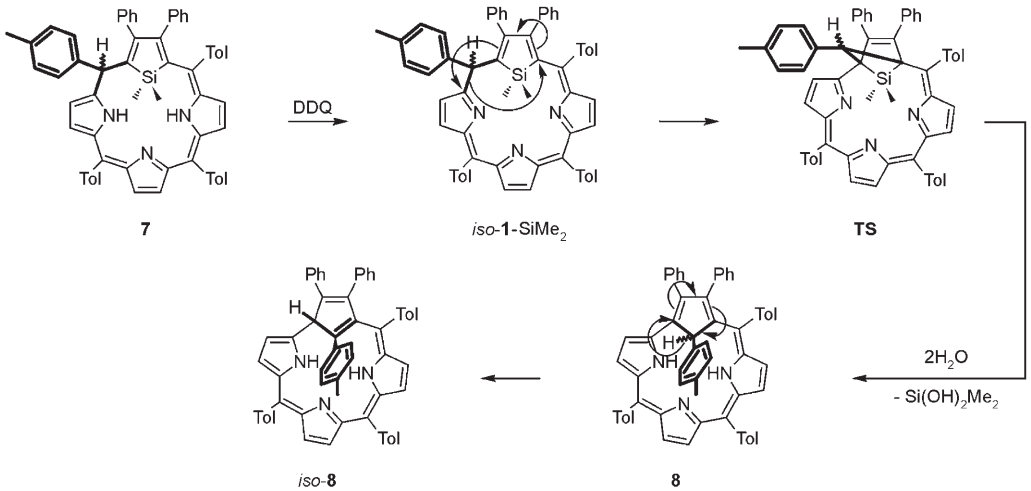

Scheme 4. Suggested ring contraction mechanism.

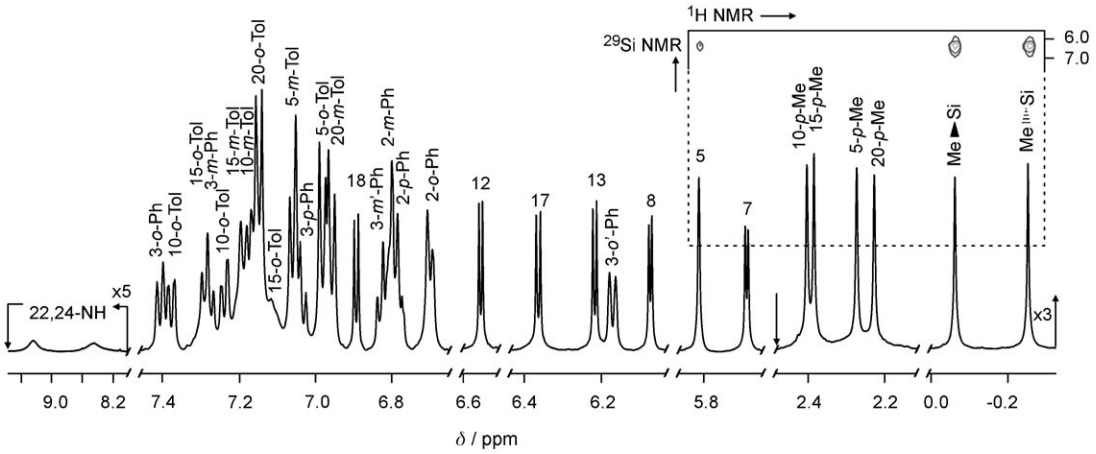

Figure 2. ^{1}H NMR spectrum of **7** ([D_2]dichloromethane, 230 K). Inset: ^{1}H,^{29}Si NMR correlations.

the β-silole position revealed different dynamic behaviour. Namely, fast rotation was detected for 2-Ph, which remains in contrast with hindered rotation seen for 3-Ph as revealed by two well-separated *o*-H doublets ($\delta = 6.18$ and 7.42 ppm, 230 K) in the entire temperature range. The marked shift difference of 3-*o*-Ph and 3-*o'*-Ph resonances is readily related to the location of the corresponding hydrogen atoms relative to the shielding zone of the adjacent 2-Ph. The structural formula of **7** (Scheme 2) demonstrated merely the projection facilitating a presentation. Non-planar structural scaffolds were considered to account for the ^{1}H NMR characteristics of **7** and *iso*-**8** (Figure 3 and Figure 6).

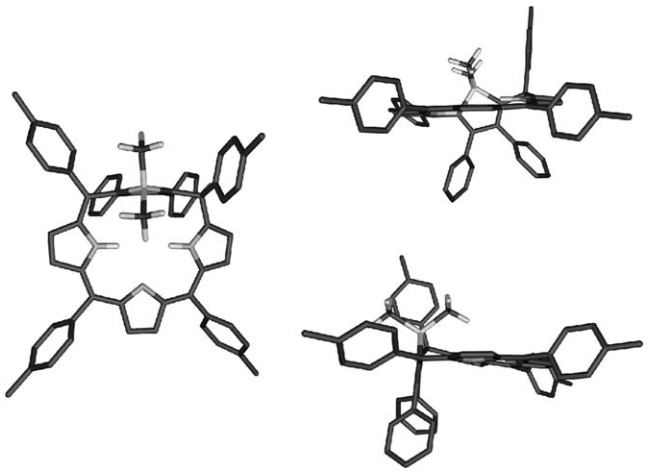

Figure 3. The DFT-optimised structure of **7** (left: perspective view; right: side views with aromatic and *p*-Me hydrogen atoms removed for clarity).

Consequently, density functional theory (DFT) studies were used to visualise the suggested structures of 21-silaphlorin and *iso*-carbacorrole and to assess the degree of macrocycle distortion that is necessary to form such macrocycles. Geometries of **7** and *iso*-**8** were optimised at the B3LYP/6-31G** level of theory. The optimised structure of **7** shows that the silole ring is nearly perpendicular to the N3 plane. Consequently, $SiMe_2$ and phenyl groups of the silole are oriented in the opposite direction being on different sides of the macrocyclic plane. The straightforward assignment of $SiMe_2$ and H5 resonances by means of ^{1}H,^{29}Si scalar coupling (Figure 2, inset) provided the initial step for the ^{1}H NMR analysis. Significantly, the complementary HMQC experiment allowed the unambiguous identification of the unique C5 resonance and revealed its tetrahedral geometry consistent with the chemical shift of 46.6 ppm. Subsequent HMBC studies revealed the cross-correlation involving *o*-H-(5-Tol)↔C5 and H5↔*o*-C(5-Tol) couples. Once assigned, this particular set of resonances was used as a starting point for the NOE studies. The fundamental relays of NOE connectivities are shown in Figure 4. The structural constraints

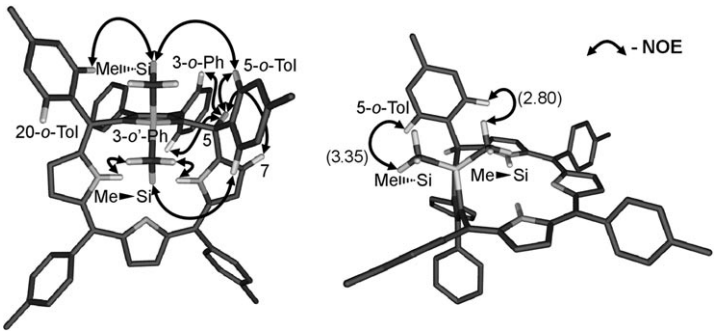

Figure 4. The established NOE connectivities for **7**. The spatial proximities [Å] are in parentheses.

determined by NOE were included in the DFT-optimised structure.

Considering in detail the spatial proximity of the Me►Si–*o*-H(5-Tol) (2.80 Å) and Me Si–*o*-H(5-Tol) (3.35 Å) as found in the DFT-optimised structure of **7** one could expect that NOE cross-peaks reflect the simultaneous dipolar coupling between both methyls of $SiMe_2$ and *o*-H(5-Tol). In

agreement with the considered structural geometry, only one methyl group Me►Si is close enough to produce the detectable dipolar 22-NH–Me►Si (2.309 Å) and 24-NH–Me►Si (2.491 Å) correlations (the shortest H–H distances are given in parentheses). The distances to hydrogen atoms of Me···Si (>5.3 Å) are too large to allow any efficient dipolar coupling. These structural features were reflected in the NOESY map by two well-defined cross-peaks (Figure S11 in the Supporting Information). The relative intensities of the NOE cross-peaks follow the expected r^{-6} relation in the series H5↔*o*-H(5-Tol) (2.466 Å) > H5↔*o*-H(3-Ph) (2.307 Å) > H5↔H7 (2.718 Å) > *o*-H(5-Tol)↔Me►Si (2.800 Å) > *o*-H(5-Tol)↔Me···Si (3.350 Å) > H5↔*o*′-H(3-Ph) (4.210 Å), thus confirming the structural analysis. Originally, two other hypothetical structural models were also considered albeit on the molecular mechanics (MM+) level only. The first one resembles **7**, but contains the 180°-rotated silole fragment. The alternative structure locates the silole ring in the tripyrrolic plane, which places the Si-methyl groups on the opposite sides of the phlorin plane. One can readily demonstrate that the above-described fundamental connectivity pattern remains in contradiction with alternative geometries. The Si-methyl groups cannot be simultaneously dipolar coupled to *o*-H(5-Tol) in any of them. It is important to note that the determined set of correlations serves as a definitive structural marker of the geometry presented in Figure 3.

The complete assignment of resonances **6** (Figures S2 and S5) confirmed the localisation of unsaturated *meso* centres as shown in Scheme 1. The structural analysis was stopped at this stage, owing to the number of feasible stereoisomers.

The spectroscopic assignment carried for *iso*-**8** (Figure 5) followed the route described in detail for **7**. The peculiar folding of the molecule is shown in the DFT-optimised structure (Figure 6).

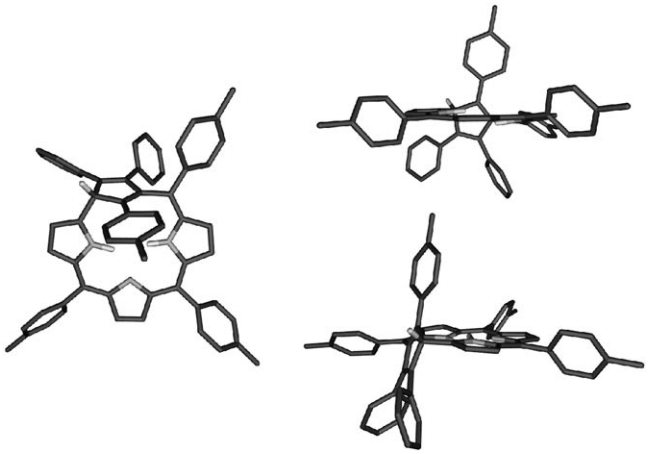

Figure 6. The DFT-optimised structure of *iso*-**8** (left: perspective view; right: side views with aromatic and Me-*p*-tolyl hydrogens removed for clarity).

The sequence of the NOE effects, starting from the structurally unique H1 resonance of *iso*-**8**, allowed determination of the rather typical relay of connectivities. It eventually afforded the complete assignment presented in Figure 5. In agreement with the tetrahedral configuration, the chemical shift of C1 equals 54.5 ppm, as confirmed by the cross-peak in the corresponding HMQC map. Significantly, a combination of HMBC and HMQC correlations (Scheme 5) permitted the identification of a cyclopentadiene skeleton.

The five ^{13}C resonances: 54.5 (C1), 141.3 (C2), 148.6 (C3), 142.3 (C4), 138.5 (C21) ppm serve as a fingerprint for the cyclopentadiene-like moiety formed during desilylation. Remarkably, the ^{13}C chemical shifts of these quintuplet carbon atoms match those of typical cyclopentadienes stabilised by aryl substitution.[65]

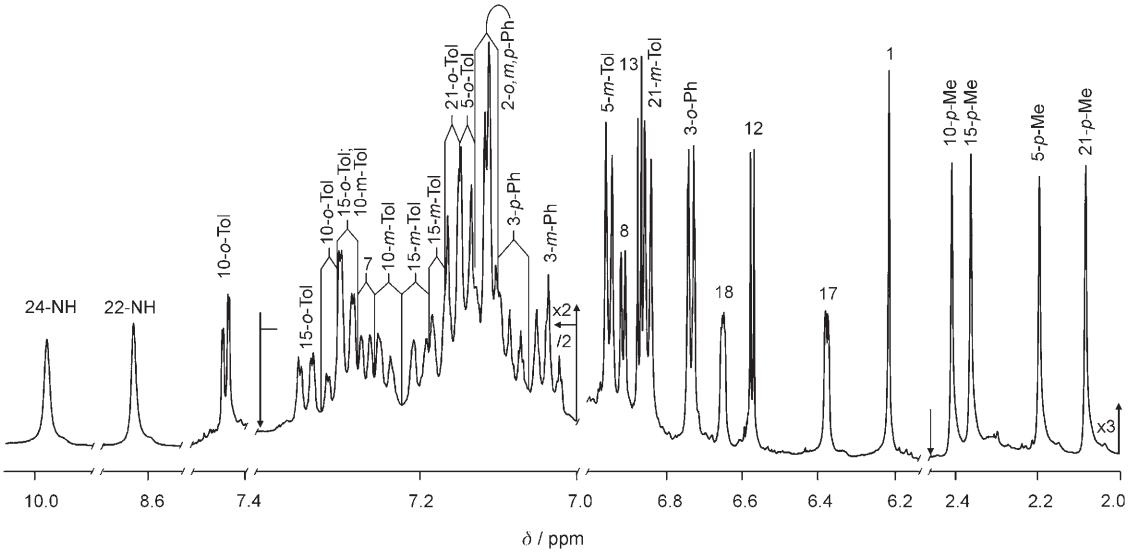

Figure 5. ^{1}H NMR spectrum of *iso*-**8** ([D_2]dichloromethane, 250 K).

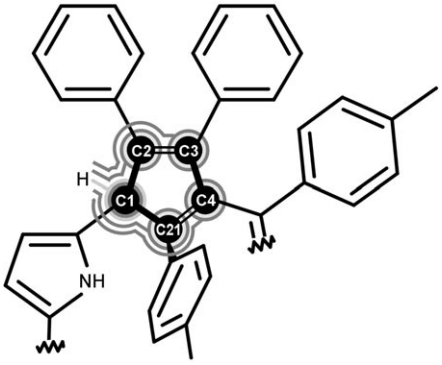

Scheme 5. HMQC and HMBC connectivities found for the cyclopentadiene moiety of *iso*-**8**.

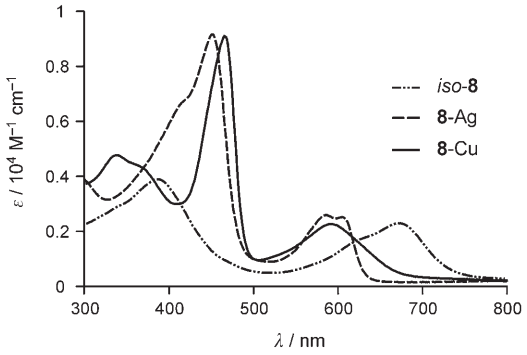

Figure 7. The electronic spectra of *iso*-**8**, **8**-Ag and **8**-Cu in dichloromethane.

Formation and characterisation of silver(III) and copper(III) carbacorroles: Reaction of silver(I) tetrafluoroborate with *iso*-carbacorrole (*iso*-**8**) in dichloromethane in the presence of triethylamine affords the green, diamagnetic, four-coordinate silver(III) carbacorrole **8**-Ag. A similar procedure using copper(II) acetate as a source of the metal ion produced the analogous copper(III) carbacorrole **8**-Cu (red-green) (Scheme 6).

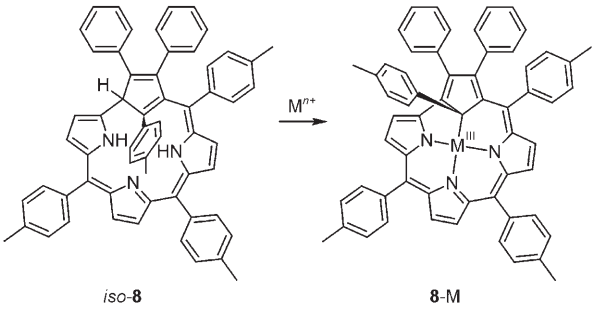

Scheme 6. Metal-ion insertion into *iso*-carbacorrole (M = Cu, Ag).

Thus the insertion process is accompanied by rearrangement of *iso*-**8** into "true" carbacorrole **8**. The macrocyclic ligand of **8**-M corresponds to the "true" carbacorrole, although it is frozen in this peculiar structure solely by coordination. The demetalation of **8**-Ag, carried out in the presence of gaseous HCl, recovers *iso*-**8**.

The electronic spectra of *iso*-**8**, **8**-Ag and **8**-Cu are shown in Figure 7. The spectrum of *iso*-**8** shows a set of bands of comparable, but relatively low intensity at $\lambda = 338$ and 386 nm, accompanied by a set of less intense bands at $\lambda =$ 624 and 673 nm. The spectra of **8**-Ag and **8**-Cu are completely different from that of the macrocyclic substrate *iso*-**8**. In particular, one can detect the intense bands in the region typically assigned to the Soret-like band of aromatic carbaporphyrinoids. Its high extinction coefficients of $\varepsilon \approx 5 \times 10^5$ suggest an aromatic character for the ligand in **8**-Ag, which remains in contrast to the UV-visible spectrum of non-aromatic *iso*-**8**. The spectroscopic pattern for **8**-Cu resembles that of **8**-Ag, although all bands exhibit a hypsochromic shift.

The ^{1}H NMR spectra of **8**-Ag and **8**-Cu differ essentially from that of *iso*-**8** (Figure 8). All pyrrole hydrogens and all *meso*-aryl hydrogens of **8**-Ag and **8**-Cu demonstrate the chemical shifts, which contain the significant downfield contribution from the aromatic ring current effect. The opposite relocation was observed for the inner tolyl ring covalently linked to the C21 carbon atom because this moiety is located in the shielding zone of the carbacorrole. The dynamically broadened resonances of 2-Ph (298 K) were detected at low temperatures (Figure 8, insets in traces A) and B), respectively). Coordination through the nitrogen donors in **8**-Ag is reflected by the presence of $^{107/109}$Ag scalar splitting seen for the β-H pyrrolic signals of H7, H8, H17 and H18. In the case of H7 and H18, $^4J_{AgH} = 1.5$ Hz (Figure 8, inset A_4), but it equals 1.1 Hz for H8 and H17. Such a coupling has not been detected for the H12 and H13 resonances of the central pyrrole ring.

Silver(III) carbacorrole dissolved in $CHCl_3$ undergoes reactions with dioxygen in the presence of aqueous HCl over a period of 48 h (Scheme 7). In the course of oxygenolysis, the benzylic C21-*p*-tolyl fragment and the silver cation are extruded. Cleavage is accompanied by formation of the furan ring as the oxygen atom replaced the C21-*p*-tolyl moiety. This eventually resulted in the formation of 2,3-diphenyl-5,10,15-tri(*p*-tolyl)-21-oxacorrole (**9**). Identification of **9** was facilitated by the fact that the analogous compound has been previously isolated and fully characterised.[66] This peculiar conversion can be compared to the transformation of 21-telluraporphyrin into 21-oxaporphyrin in the presence of dioxygen.[8]

Crystal structure of 8-Ag: The structure of silver(III) carbacorrole was determined by X-ray crystallography. The perspective views of the molecule are given in Figure 9, which shows that the macrocycle is distorted from planarity. The tetrahedral geometry around the C21 atom is demonstrated by the values of the respective bond angles. Table 1 contains selected bond lengths and angles.

The Ag–N and Ag–C bond lengths (Table 1) are comparable to those in other silver(III) carbaporphyrinoids: sil-

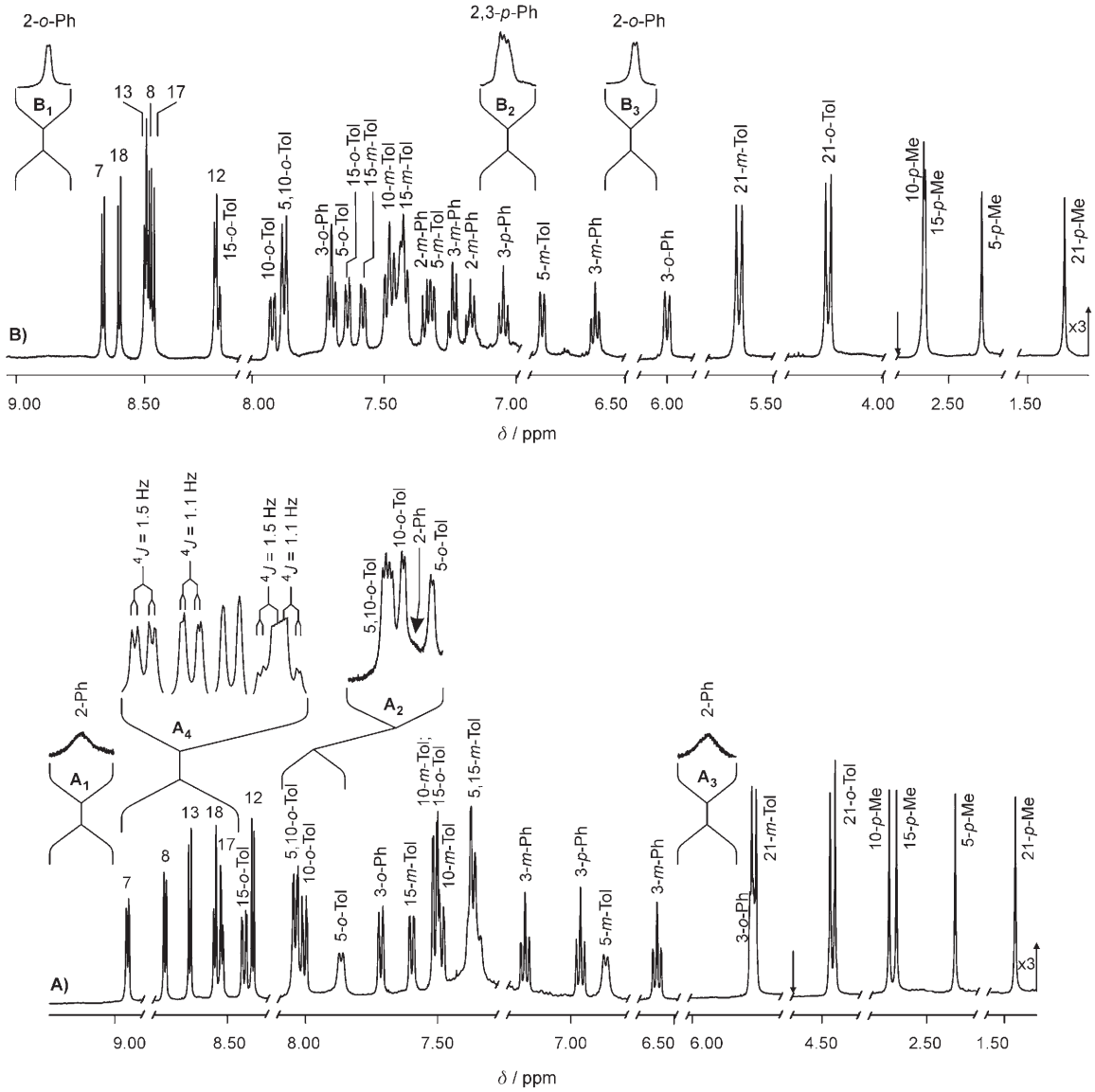

Figure 8. ^{1}H NMR spectra of: A) **8**-Ag ([D]chloroform, 250 K) and B) **8**-Cu ([D_2]dichloromethane, 250 K). Insets A_1, A_2, A_3 show 2-Ph signals observed at 210 K; Inset A_4 shows $^{107/109}$Ag scalar splitting, 298 K. Insets B_1, B_2, B_3 show 2-Ph signals observed at 180 K.

ver(III) inverted porphyrin [Ag–N22, 2.06(2); Ag–N23, 2.08(2); Ag–N24, 2.03(2); and Ag–C21, 2.04(2)],[67] silver(III) benzocarbaporphyrin [Ag–N22, 2.038(4); Ag–N23, 2.084(4); Ag–N24, 2.046(4); Ag–C21, 2.015(4)],[68] silver(III) double *N*-confused porphyrin [Ag–C21, 2.011(7); Ag–C22, 1.987(2); Ag–N23, 2.064(5); and Ag–N24, 2.047(7)],[69] silver(III) *O*-confused oxaporphyrin with appended pyrrole ring [Ag–N22, 2.031(5); Ag–N23, 2.069(5); Ag–N24, 2.042(5); Ag–C21, 2.020(7)],[19] and silver(III) carabaporpholactone [Ag–C21, 2.013(5); Ag–N22, 2.020(4); Ag–N23, 2.038(4); Ag–N24, 2.039 (4)].[17] A comparison of the structural data, although limited to the five available examples of silver(III) (NNNC) carbaporphyrinoids, shows that silver(III)–carbon(sp^3) and silver(III)–carbon(sp^2) bond lengths are very similar in spite of the different nature of the carbon donors.

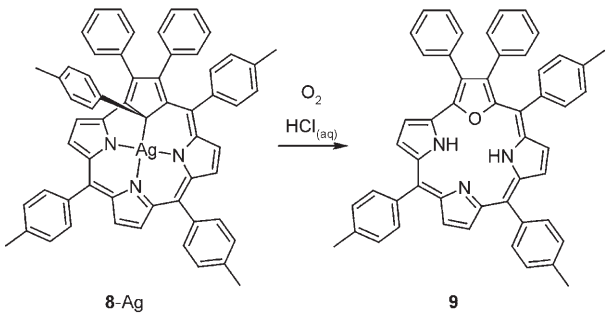

Scheme 7. Reaction of **8**-Ag with dioxygen.

DFT calculations: One question requiring an answer is why the oxidation of 21-silaphlorin leads to a *iso*-carbacorrole

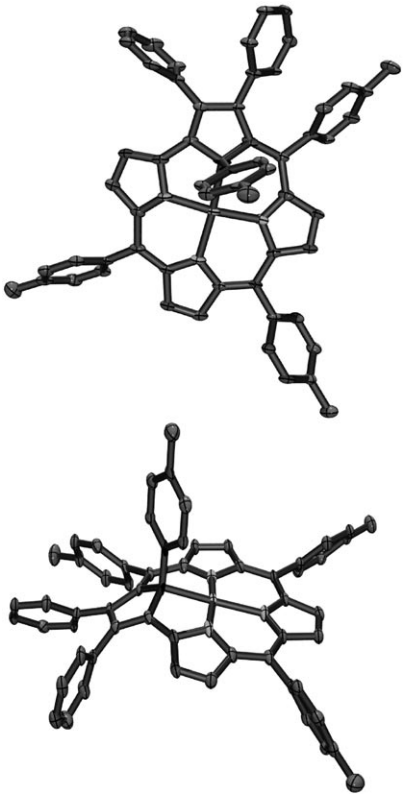

Figure 9. The crystal structure of **8**-Ag (top: perspective view; bottom: side view with hydrogen atoms omitted for clarity). The thermal ellipsoids represent 50% probability.

Table 1. Selected bond lengths and angles.

Bond lengths	[Å]	Angles	[°]
Ag–C21	2.046(5)	Ag–C21–C1	104.5(4)
Ag–N22	1.986(5)	Ag–C21–C4	113.6(4)
Ag–N23	2.025(4)	Ag–C21–C_{ipso}	102.3(3)
Ag–N24	1.984(5)	C1–C21–C_{ipso}	116.4(5)
		C1–C21–C4	105.4(4)
		C4–C21–C_{ipso}	114.5(5)

structure *iso*-**8** instead of the alternative isomeric structures: regular carbacorrole **8**, 4-*iso*-carbacorrole 4-*iso*-**8**, (*R*)-5-*iso*-carbacorrole (*R*)-5-*iso*-**8**, (*S*)-5-*iso*-carbacorrole (*S*)-5-*iso*-**8**, vacataporphyrin **10** or cyclobutadienephlorin **11**.

One reasonable hypothesis is that a steric relief allowed by a *iso*-carbacorrole ring drives the conversion. We carried out DFT calculations to address this problem. DFT was successfully used to describe the properties of porphyrins and related systems, providing information on their energetics, conformational behaviour, tautomerism and aromaticity.[70] We have previously applied DFT modelling to study the relationships between aromaticity, tautomerism, and coordinating capabilities of carbaporphyrinoids.[18,71–76] In particular, we were able to reproduce the energetic preference of vacataporphyrin for a strictly planar conformation.[10] In analogy to an unorthodox geometry of 21,23-ditellurapor-

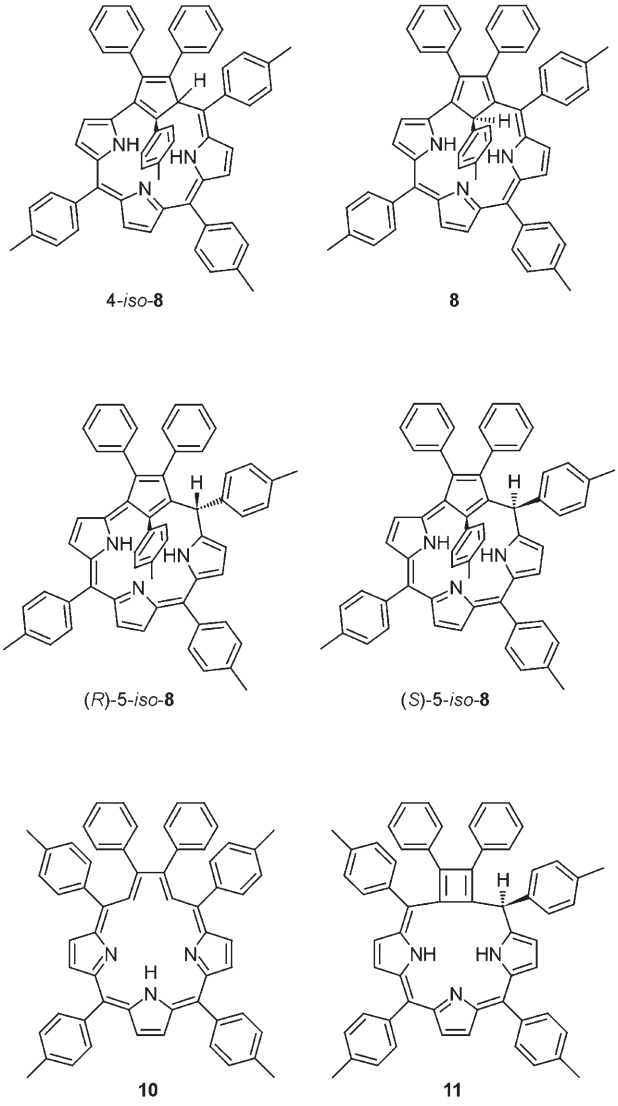

phyrin,[11] the inverted geometry of the free ligand was considered as well.

The optimised structures are shown in Figure 10. The total energies, calculated at the B3LYP/6-31G**//B3LYP/6-31G** level (Table 2), readily demonstrated that *iso*-carbacorrole is the most stable. The relative energies of isomers increase in the order: *iso*-carbacorrole < carbacorrole < vacataporphyrin < cyclobutadienephlorin. In our opinion, this analysis provides some additional insight into the coordinat-

Table 2. The calculated total energies (B3LYP/6-31G**//B3LYP/6-31G**).

Compound	Number	Energies [kcal mol^{-1}] vs. *iso*-**8**
iso-carbacorrole	*iso*-**8**	0.00
carbacorrole	**8**	2.60
4-*iso*-carbacorrole	4-*iso*-**8**	10.86
(*R*)-5-*iso*-carbacorrole	(*R*)-5-*iso*-**8**	15.30
(*S*)-5-*iso*-carbacorrole	(*S*)-5-*iso*-**8**	17.40
vacataporphyrin	**10**	20.86
cyclobutadienephlorin	**11**	52.79

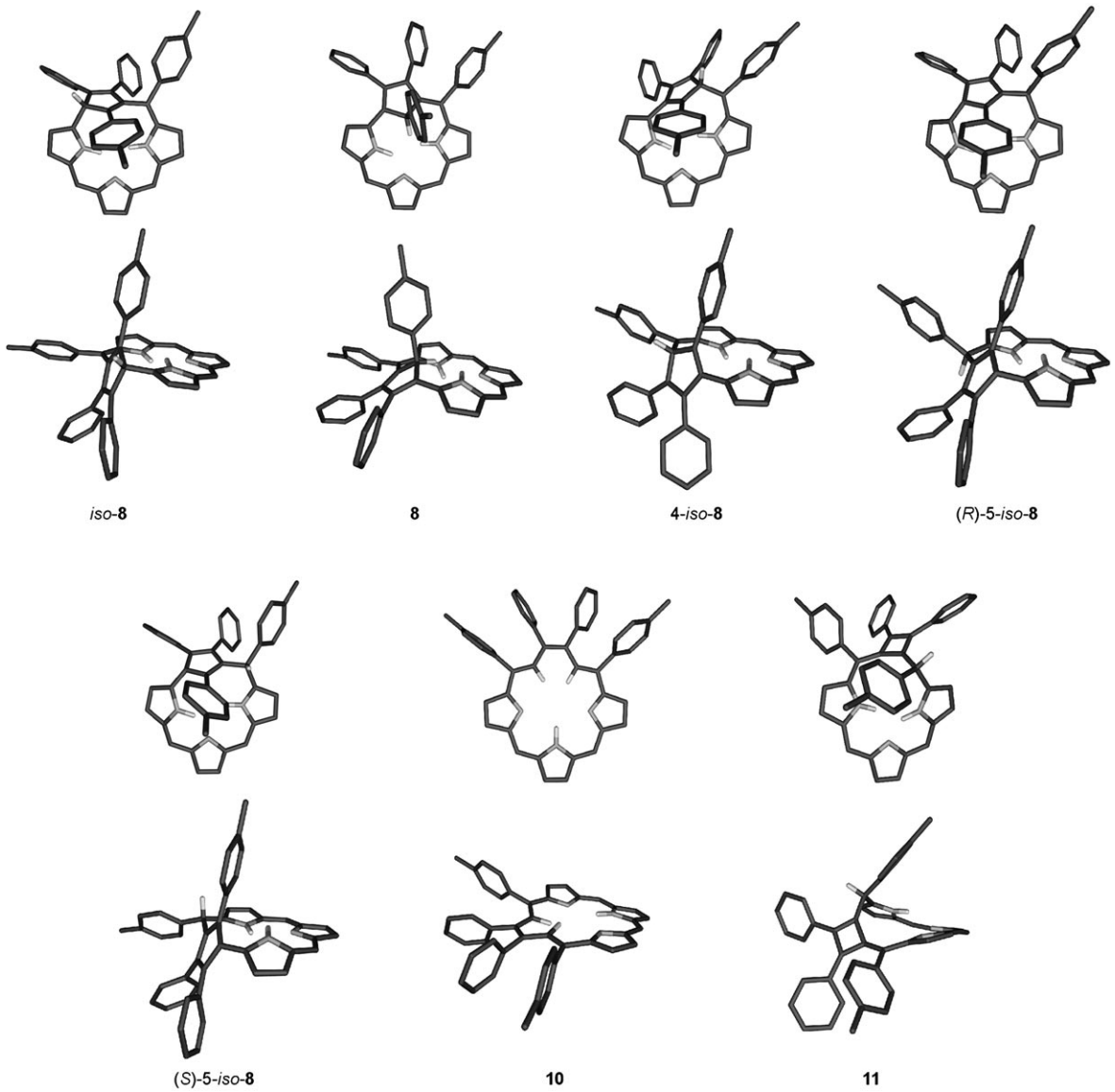

Figure 10. The DFT-optimised structures of *iso*-**8**, **8**, 4-*iso*-**8**, (*R*)-5-*iso*-**8**, (*S*)-5-*iso*-**8**, **10**, **11** (top: perspective views; bottom: side views with aromatic, *p*-Me hydrogen atoms and 10,15-*p*-tolyl groups removed for clarity).

ing properties of carbacorrole. Previously, considering the mechanism of metal-ion insertion into the coordination core of inverted porphyrin or 2-oxybenziporphyrin, we included a preorganisation step into the mechanistic route.[71,77] Thus, in order to satisfy the requirements imposed by the inserted metal ion, the molecular and electronic structures of the ligand have to be prearranged, contributing to the overall activation energy of metal insertion. For instance, preorganisation energies for *iso*-**8**→**8** or **8**→**10** are relatively small in comparison to activation energies determined for insertion of a metal ion into porphyrins and *N*-methylporphyrins.[78–81] This leads us to expect that carbacorrole will coordinate using several different coordination modes, depending on the nature of the central atom.

Conclusion

21-Silaphlorin is a new heteroporphyrinoid, which is related to phlorin derived from the [18]porphyrin(1.1.1.1) frame and contains a silole ring that replaces one of the pyrroles. 21-Silaphlorin reveals a remarkable reactivity that involves the extrusion of a silylilene unit followed by intramolecular rearrangements to form a non-aromatic *iso*-carbacorrole ring. Interestingly, considering the macrocyclic frame the *iso*-carbacorrole on its own, carbacorrole and cyclobutadieneporphyrin are readily recognised as constitutional isomers of vacataporphyrin (butadieneporphyrin).[10] The *iso*-carbacorrole, applied as a ligand to silver(III) or copper(III) ions, reveals the peculiar plasticity of its molecular and electronic structure. The structural changes are triggered by the

tetrahedral–trigonal rearrangements at the C1 atom accompanied by trigonal–tetrahedral rearrangement at the inner C21 carbon atom. Such a prearrangement is necessary to allow a formation of a metal(III)–carbon(sp^3) σ bond. Thus coordination of copper(III) or silver(III) provides a noteworthy route to trap a rare aromatic carbacorrole structure. Formally, such a molecule can be constructed by the replacement of the pyrrole ring in triarylcorrole by a cyclopentadiene moiety.

Experimental Section

Instrumentation: NMR spectra were recorded on a Bruker Avance 500 MHz spectrometer. Absorption spectra were recorded by means of a Varian Cary 50 Bio spectrometer. Mass spectra were recorded by means of a Bruker micrOTOF-Q and AD-604 spectrometers by using the electrospray, liquid-matrix secondary-ion mass spectrometry and electron-impact techniques.

X-ray analysis: X-ray-quality crystals of **8**-Ag were prepared by diffusion of methanol into a solution of **8**-Ag in dichloromethane in a thin tube. Data were collected at 100 K on a Kuma KM-4 CCD diffractometer. The data were corrected for Lorentz and polarisation effects. An analytical absorption correction was applied. Crystal data are compiled in Table 3. The structure was solved by direct methods by using SHELXS-97 and refined by the full-matrix least-squares method by SHELXL-97 with anisotropic thermal parameters for non-hydrogen atoms.[82,83]

Table 3. Crystallographic data for **8**-Ag.

	8-Ag
solvent of crystallisation	MeOH into CH_2Cl_2
empirical formula	$C_{60}H_{44}N_3Ag$
T[K]	100(2)
crystal system	monoclinic
space group	$P2(1)/n$
V[Å^3]	4919.8(2)
a[Å]	14.0223(4)
b[Å]	16.7096(3)
c[Å]	21.9074(5)
α[°]	90
β[°]	106.575(3)
γ[°]	90
Z	4
ρ_{calcd}[g cm^{-3}]	1.415
θ range	$4.12 \leq \theta \leq 38.59$
hkl range	$-16 \leq h \leq 16$
	$-19 \leq k \leq 19$
	$-23 \leq l \leq 26$
GoF (F^2)	0.914
R_1	0.0615
wR_2	0.1804

CCDC-671119 contains the supplementary crystallographic data for this paper. These data can be obtained free of charge from The Cambridge Crystallographic Data Centre via www.ccdc.cam.ac.uk/data_request/cif.

Computational chemistry: Density functional theory calculations were performed by using Gaussian 03.[84] Geometry optimisations were carried out within unconstrained $C1$ symmetry, with starting coordinates preoptimised with semiempirical methods. Becke's three-parameter exchange functional[85] with the gradient-corrected correlation formula of Lee, Yang, and Parr (B3LYP)[86] was used with the 6-31G** basis set.

Materials: Tetrahydrofuran, dichloromethane and pyrrole were purified by standard procedures. *p*-Tolylaldehyde (Aldrich) was used as received.

1,1-Dimethyl-3,4-diphenyl-2,5-bis(*p*-tolylhydroxymethyl)silole (5): *p*-Tolylaldehyde (3.06 mL, 26 mmol) was added to the vigorously stirred solution of 2,5-dilithium-3,4-diphenyl-1,1-dimethylsilole[32–34] (6.50 mmol) in tetrahydrofuran (60 mL) at −78 °C under nitrogen. The mixture was stirred for 1 h, and then the reaction flask was taken out from the cooling bath and left until it reached room temperature. The mixture was poured into water (50 mL). The organic products were extracted with diethyl ether (3×25 mL). The combined extract was washed with brine, dried over $MgSO_4$, filtered, and evaporated under reduced pressure. The residue was dissolved in dichloromethane/hexane (0.5:9.5 v/v) and purified by column chromatography (silica gel 70–230, 100 g). The first colourless fraction was naphthalene. The second orange fraction eluted with dichloromethane was collected. Recrystallisation from toluene gave enantiomers **5**-*SS* (*RR*) as a white powder (1.5 g, 3.0 mmol). The third orange fraction contained benzyl alcohol. The last fraction (orange) eluted with methanol/dichloromethane (0.3:9.7 v/v) was collected. The solvent was removed on a rotary evaporator. The residue was diluted with hexane, and insoluble materials were filtered out. The filtrate was condensed to afford **5**-*RS* as an orange oil (1.2 g, 2.4 mmol). Total yield: 83%; HRMS (ESI): m/z calcd for $C_{34}H_{33}OSi^+$: 485.2301, found: 485.2280 $[M-OH]^+$.

Compound **5**-SS *(*RR*)*: ^{1}H NMR ($CDCl_3$, 230 K): $\delta = 7.18$ (t, 2H; 3,4-*m*-Ph), 7.10 (d, 2H; 3,4-*o*-Ph), 7.07 (m, 2H; 3,4-*p*-Ph), 7.06 (d, 4H; 1,6-*m*-Tol), 7.03 (d, 6H; 1,6-*m*-Tol, 3,4-*m*′-Ph), 6.68 (d, 2H; 3,4-*o*′-Ph), 5.44 (s, 2H; 1,6), 2.29 (s, 6H; 1,6-*p*-Me), 1.85 (s, 2H; OH), −0.13 ppm (s, 6H; Me−Si); ^{13}C NMR ($CDCl_3$, 230 K): $\delta = 154.2$ (3,4), 143.7 (2,5), 140.9 (C_1–1,6-Tol), 138.0 (C_1–3,4-Ph), 136.7 (C_4–1,6-Tol), 129.3 (3,4-*o*′-Ph), 129.0 (3,4-*o*-Ph, 1,6 *m*-Tol), 127.9 (3,4-*m*-Ph), 127.8 (3,4-*m*′-Ph), 126.8 (3,4-*p*-Ph), 125.6 (1,6-*o*-Tol), 73.0 (1,6), 21.6 (1,6-*p*-Me), −2.4 ppm (Me−Si); ^{29}Si NMR ($CDCl_3$, 298 K): $\delta = 6.22$ ppm.

Compound **5**-RS: ^{1}H NMR ($CDCl_3$, 230 K): $\delta = 7.01$ (m, 6H; 3,4-*m*-Ph, 3,4-*p*-Ph), 7.05 (d, 4H; 1,6-*m*-Tol), 7.03 (2H; 4-*o*-Ph), 7.01 (d, 4H; 1,6-*o*-Tol), 6.81 (d, 2H; 3-*o*-Ph), 5.40 (s, 2H; 1,6), 2.23 (s, 3H; 1,6-*p*-Me), 0.50 (s, 3H; Me|||·Si), −0.85 ppm (s, 3H; Me►Si); ^{13}C NMR ($CDCl_3$, 230 K): $\delta = 154.0$ (3,4), 143.4 (2,5), 140.9 (C_1–1,6-Tol), 137.8 (C_1–3,4- Ph), 136.4 (C_4–1,6-Tol), 129.2 (3-*o*-Ph), 129.0 (4-*o*-Ph), 128.7 (1,6-*o*-Tol), 127.7, 127.5 (3,4-*m*-Ph), 126.6 (3,4-*p*-Ph), 125.5 (1,6-*m*-Tol), 72.6 (1,6), 21.3 (1,6-*p*-Me), −2.3 (Me|||·Si), −2.8 ppm (Me►Si); ^{29}Si NMR ($CDCl_3$, 298 K): $\delta =$ 6.18 ppm.

Dihydro-21-silaphlorin (6): A 500 mL round-bottomed flask equipped with a stirring bar, topped with a tube filled with $CaCl_2$ and a nitrogen inlet, was charged with freshly distilled dichloromethane (450 mL). 2,5-Bis(*p*-tolylhydroxymethyl)-3,4-diphenyl-1,1-dimethylsilole (**5**, 0.5 g, 1 mmol), pyrrole (0.21 mL, 3 mmol), *p*-tolylaldehyde (0.24 mL, 2 mmol) and triethyl orthoformate (0.21 mL, 1.25 mmol) were added and the solution was purged with nitrogen for 20 min at room temperature. Subsequently, $BF_3{\cdot}Et_2O$ (0.158 mL, 1.25 mmol) was added. The reaction mixture was protected from light. After 1 h of stirring at room temperature, DDQ (0.681 g, 3 mmol) was added and stirring was continued for a further 5 min. The solvent was removed by means of a vacuum rotary evaporator. The dark residue was dissolved in dichloromethane and subjected to preliminary chromatographic separation on a short basic alumina (grade II) column. The fast-moving fraction was collected and separated again by chromatography on a basic alumina (grade II) column using a mixture of dichloromethane/hexane (from 1:9 to 5:5 v/v) as the eluent. Compound **6** eluted first as a yellow fraction preceded by a small amount of a greenish impurity. The crude product was further purified by column chromatography on a basic alumina (grade II, dichloromethane/hexane 1.5:8.5 v/v). Yield of **6** varied from traces to 9 mg (1%). Compound **7** eluted second as a green fraction and was often contaminated with $TTPH_2$ ($TTPH_2$ = 5,10,15,20-tetra-*p*-tolylporphyrin). The mixture of macrocyclic products was further purified by column chromatography on a basic alumina (grade II, dichloromethane/hexane 2:8 v/v). Yield of **7**: 9 mg (1%), ^{1}H NMR ($CDCl_3$, 230 K): $\delta = 11.66$ (br s, 1H; 24-NH), 7.81(s, 1H; 22-NH), 7.42 (m, 1H; 2-*m*-Ph), 7.41(2d, 2H; 15-*o*-Tol), 7.39 (d, 1H; 2-*o*-Ph), 7.37 (2d, 2H; 10-*o*-Tol), 7.27 (m, 5H; 3-*m*-Ph, 5-*o*-Tol, 15-*m*-Tol), 7.21 (m. 2H; 2-*p*-Ph, 3-*o*-Ph), 7.16 (d, 2H; 10-*m*-Tol), 7.09 (d, 2H; 5-*m*-Tol), 7.08 (d, 1H; 2-*m*-Ph), 7.02 (m, 1H; 3-*p*-Ph), 6.94 (d, 2H; 20-*m*-Tol), 6.78 (d, 2H; 20-*o*-Tol), 6.67 (d, 1H; 13), 6.63 (d, 1H; 2-*o*-Ph), 6.48

(m, 1H; 3-*m*-Ph), 6.42 (d, 1H; 12), 6.36 (d, 1H; 17), 6.04 (m, 1H; 8), 5.87 (d, 1H; 18), 5.56 (m, 1H; 7), 5.48 (s, 1H; 10), 5.47 (d, 1H; 3-*o*-Ph), 5.14 (s, 1H; 20), 4.67 (s, 1H; 5), 2.42 (s, 3H; 15-*p*-Me), 2.30 (s, 3H; 10-*p*-Me), 2.26 (s, 3H; 5-*p*-Me), 2.18 (s, 3H; 20-*p*-Me), 0.01 (s, 3H; Me►Si), −1.16 ppm (s, 3H; Me|||·Si); ^{13}C NMR ($CDCl_3$, 230 K): δ = 154.7 (2), 151.5 (3), 146.5 (4), 141.5 (1), 140.1 (15), 139.4 (C_1–20-Tol), 138.6 (C_4–15-Tol), 138.3 (C_1–2-Ph), 137.9 (C_1–10-Tol), 137.6 (C_1–5-Tol), 137.4 (C_1–3-Ph), 136.4 (C_4–5-Tol), 136.3 (C_4–10-Tol, C_4–20-Tol), 135.0 (C_1–15-Tol), 134.5 (13), 133.9 (16), 130.9 (6), 130.8 (2-*m*-Ph), 130.6 (9), 129.8 (3-*o*-Ph), 129.7 (10-*m*-Tol), 129.3 (10-*o*-Tol, 19), 129.0 (5-*m*-Tol), 128.9 (20-*m*-Tol), 128.8 (20-*o*-Tol), 128.7 (5-*o*-Tol), 128.6 (2-*o*-Ph, 3-*o*-Ph), 128.5 (3-*m*-Ph),128.2 (14, 15-*m*-Tol), 128.0 (11), 127.9 (2-*o*-Ph, 15-*o*-Tol), 127.8 (2-*m*-Ph), 127.4 (3-*m*-Ph), 126.9 (2-*p*-Ph), 126.4 (2-*p*-Ph), 125.7 (17), 123.2 (12), 113.4 (18), 106.7 (8), 104.2 (7), 47.0 (20), 45.4 (10), 45.3 (5), 21.3 (15-*p*-Me), 21.0 (10-*p*-Me; 20.9 (5-*p*-Me), 20.8 (20-*p*-Me), −2.9 (Me►Si), −3.9 ppm (Me|||·Si); ^{29}Si NMR ($CDCl_3$, 298 K): δ = 5.79 ppm; HRMS (ESI): *m*/*z* calcd for $C_{62}H_{56}N_3Si^+$: 870.4243, found: 870.4183 $[M+H]^+$; UV/Vis (CH_2Cl_2, 298 K): $\lambda_{max}(\log\varepsilon)$ = 316 (5.15), 453 (5.20) 687 nm (3.93 $M^{-1}cm^{-1}$).

21-Silaphlorin (7): See the procedure for **6**. ^{1}H NMR (CD_2Cl_2, 230 K): δ = 9.20, 8.41 (br, 2 s, 2H; 22,24-NH), 7.42 (d, 1H; 3-*o*-Ph), 7.39, 7.25 (2d, 2H; 10-*o*-Tol), 7.31, 7.12 (2d, 2H; 15-*o*-Tol), 7.29 (m, 1H; 3-*m*-Ph), 7.20 (d, 2H; 15-*m*-Tol), 7.18 (d, 2H; 10-*m*-Tol), 7.16 (2d, 2H; 20-*o*-Tol), 7.08 (d, 2H; 5-*m*-Tol), 7.06 (m, 1H; 3-*p*-Ph), 6.99 (d, 2H; 5-*o*-Tol), 6.97 (d, 2H; 20-*m*-Tol), 6.91 (d, 1H; 18), 6.84 (m, 1H; 3-*m*′-Ph), 6.81 (d, 2H; 2-*m*-Ph), 6.79 (m, 1H; 2-*p*-Ph), 6.71 (d, 2H; 2-*o*-Ph), 6.57 (d, 1H; 12), 6.37 (d, 1H; 17), 6.23 (d, 1H; 13), 6.18 (d, 1H; 3-*o*′-Ph), 6.09 (d, 1H; 8), 5.81 (s, 1H; 5), 5.69 (d, 1H; 7), 2.38 (s, 3H; 10-*p*-Me), 2.37 (s, 3H; 15-*p*-Me), 2.26 (s, 3H; 5-*p*-Me), 2.21 (s, 3H; 20-*p*-Me), −0.05 (s, 3H; Me►Si), −0.24 ppm (s, 3H; Me|||·Si); ^{13}C NMR (CD_2Cl_2, 230 K): δ = 167.6 (14), 159.8 (2), 154.3 (3), 151.5 (11), 145.5, 142.2 (16, 19), 142.4 (1), 140.5 (C_1–5-Tol), 139.4 (6), 138.2 (C_1–2-Ph), 137.9 (C_1–15-Tol), 137.9 (C_1–3-Ph), 137.7 (C_4–10-Tol), 136.55 (C_4–5-Tol), 136.5 (C_4–15-Tol, C_4–20-Tol), 135.9 (12), 135.3 (4), 135.2 (C_1–20-Tol), 133.2 (C_1–10-Tol), 132.6 (9), 132.1 (10, 15-*o*-Tol), 131.5 (10-*o*-Tol), 129.1 (5-*m*-Tol), 128.8 (20-*m*-Tol), 128.7 (3-*o*-Ph, 20-*o*-Tol), 128.6 (13, 15-*m*-Tol), 128.3 (2-*o*-Ph), 128.2 (3-*o*′-Ph), 128.1 (17), 128.0 (5-*o*-Tol), 127.9 (3-*m*-Ph), 127.8 (10-*m*-Tol), 127.6 (3-*m*′-Ph), 126.8 (2-*p*-Ph), 126.6 (3-*p*-Ph), 126.5 (18), 126.4 (2-*m*-Ph), 123.1 (8), 121.9 (20), 110.7 (7), 107.8 (15), 46.6 (5), 21.3 (10-*p*-Me), 21.2 (15-*p*-Me), 21.1 (20-*p*-Me; 21.0 (5-*p*-Me), −2.6 (Me|||·Si), −3.2 ppm (Me►Si); ^{29}Si NMR (CD_2Cl_2, 298 K): δ = 6.52; HRMS (ESI): *m*/*z* calcd for $C_{62}H_{54}N_3Si^+$: 868.4087, found: 868.4104 $[M+H]^+$; UV/Vis (CH_2Cl_2, 298 K): $\lambda_{max}(\log\varepsilon)$ = 315 (5.22), 404 (5.44), 647 (5.14), 697 nm (5.28 $M^{-1}cm^{-1}$).

***iso*-Carbacorrole (*iso*-8)**: A 500 mL round-bottomed flask equipped with a stirring bar and nitrogen inlet, was charged with freshly distilled dichloromethane (450 mL). 2,5-Bis(*p*-tolylhydroxymethyl)-3,4-diphenyl-1,1-dimethylsilole (**5**, 0.5 g, 1 mmol), pyrrole (0.21 mL, 3 mmol), *p*-tolylaldehyde (0.24 mL, 2 mmol) and water (0.036 mL, 2 mmol) were added and the solution was purged with nitrogen for 20 min at room temperature. The reaction mixture was protected from light and $BF_3{\cdot}Et_2O$ (0.158 mL, 1.25 mmol) was added. After 1 h of stirring at room temperature, DDQ (0.908 g, 4 mmol) was added and stirring was continued for a further 5 min. The solvent was removed with a vacuum rotary evaporator. The dark residue was dissolved in dichloromethane and subjected to preliminary chromatography separation on a short basic alumina (grade II) column. The fast-moving fraction was collected and separated again by chromatography on a basic alumina (grade II) column using as the eluent a mixture of dichloromethane/hexane (3:7 v/v). *iso*-**8** eluted first as a see-green fraction. The crude product was further purified by column chromatography basic alumina (grade II, dichloromethane/hexane 1.5:8.5 v/v). Yield of *iso*-**8**: 8 mg (1%), ^{1}H NMR (CD_2Cl_2, 250 K): δ = 9.98 (s, 1H; 24-NH), 8.64 (s, 1H; 22-NH), 7.47, 7.33 (2d, 2H; 10-*o*-Tol), 7.36 (d, 1H; 15-*o*-Tol), 7.31 (d, 2H; 15-*o*-Tol, 10-*m*-Tol), 7.28 (d, 1H; 7), 7.26 (d, 1H; 10-*m*-Tol), 7.22, 7.19 (2d, 2H; 15-*m*-Tol), 7.17 (d, 2H; 21-o-Tol), 7.16 (d, 2H; 5-*o*-Tol), 7.14–7.11 (m, 5H; 2-*o*,*m*,*p*-Ph), 7.10 (t, 1H; 3-*p*-Ph), 7.05 (t, 2H; 3-*m*-Ph), 6.96 (d, 2H; 5-*m*-Tol), 6.93 (d, 1H; 8), 6.88 (d, 1H; 13), 6.86 (d, 2H; 21-*m*-Tol), 6.75 (d, 2H; 3-*o*-Ph), 6.66 (m, 1H; 18), 6.59 (d, 1H; 12), 6.39 (d, 1H; 17), 6.23 (s, 1H; 1), 2.44 (s, 3H; 10-*p*-Me), 2.39 (s, 3H; 15-*p*-Me), 2.23 (s, 3H; 5-*p*-Me), 2.12 ppm (s, 3H; 21-*p*-Me); ^{13}C NMR (CD_2Cl_2, 250 K): δ = 165.8 (11), 150.6 (14), 148.6 (3), 146.3 (9), 142.7 (6), 142.3 (4), 141.3 (2), 138.5 (21), 138.3 (C_4–15-Tol), 137.5 (C_4–21-Tol), 137.0 (C_4–5-Tol), 136.9 (C_4–10-Tol), 136.3 (C_1–10-Tol), 135.9 (C_1–3-Ph), 135.6 (19), 135.4 (C_1–2-Ph), 135.3 (C_1–15-Tol), 135.0 (C_1–5-Tol), 134.6 (13), 132.7 (16), 132.3 (15), 132.3 (10-*o*-Tol), 132.0 (10-*o*-Tol, 15-*o*-Tol), 131.3 (15-*o*-Tol), 130.7 (C_1–21-Tol), 130.3 (8), 128.5 (21-*m*-Tol), 129.2 (5-*o*-Tol), 129.1 (3-o-Ph, 5-*m*-Tol), 129.0 (2-*o*-Ph), 128.84, 128.81 (10-*m*-Tol), 128.4 (15-*m*-Tol), 128.3 (2-*m*-Ph, 15-*m*-Tol), 128.1 (3-*m*-Ph), 127.6 (21-*o*-Tol), 127.4 (12), 127.1 (2-*p*-Ph, 3-*p*-Ph), 126.9 (7), 120.3 (17), 116.5 (5), 112.1 (18), 108.7 (10), 54.5 (1), 21.4 (15-*p*-Me), 21.3 (10-*p*-Me), 21.2 (5-*p*-Me), 21.1 ppm (21-*p*-Me); HRMS (EI): *m*/*z* calcd for $C_{60}H_{47}N_3$: 809.3770, found: 809.3771 $[M]^+$; UV/Vis (CH_2Cl_2, 298 K): $\lambda_{max}(\log\varepsilon)$ = 338 (5.90), 386 (5.99), 624 (5.58) 673 nm (5.74 $M^{-1}cm^{-1}$).

Silver(III) carbacorrole (8-Ag): Compound *iso*-**8** (16 mg, 0.02 mmol) was dissolved in freshly distilled dichloromethane (20 mL), than excess $AgBF_4$ was added. The solution turned immediately from sea-green to red. The resulting mixture was stirred for 5 min, and then TEA (excess) was added. The colour changed to green. The mixture was directly moved to the top of column chromatography on a silica gel (mesh 70–230). The first green band moving with dichloromethane was collected and evaporated to dryness. The residue contains practically pure **8**-Ag complex. Yield: 16.4 mg (90%), ^{1}H NMR ($CDCl_3$, 230 K): δ = 9.19, 7.89, 5.91 (br, 3 s, 5H; 2-Ph, 210 K), 8.95 (d, 1H; 7), 8.72 (d, 1H; 8), 8.63 (d, 1H; 13), 8.54 (d, 1H; 18), 8.51 (d, 1H; 17), 8.43 (d, 1H; 15-*o*-Tol), 8.40 (d, 1H; 12), 8.04 (d, 2H; 5-*o*-Tol, 10-*o*-Tol), 8.00 (d, 1H; 10-*o*-Tol), 7.87 (d, 1H; 5-*o*-Tol), 7.72 (d, 1H; 3-*o*-Ph), 7.61 (d, 1H; 15-*m*-Tol), 7.52 (d, 2H; 10-*m*-Tol, 15-*o*-Tol), 7.50 (d, 1H; 10-*m*-Tol), 7.38 (m, 2H; 5-*m*-Tol, 15-*m*-Tol), 7.16 (t, 1H; 3-*m*-Ph), 6.96 (m, 1H; 3-*p*-Ph), 6.87 (d, 1H; 5-*m*-Tol), 6.55 (t, 1H; 3-*m*-Ph), 5.76 (d, 1H; 3-*o*-Ph), 5.75 (d, 2H; 21-*m*-Tol), 4.46 (d, 2H; 21-*o*-Tol), 2.64 (s, 3H; 10-*p*-Me), 2.61 (s, 3H; 15-*p*-Me), 2.39 (s, 3H; 5-*p*-Me), 1.46 ppm (s, 3H; 21-*p*-Me); ^{13}C NMR ($CDCl_3$, 230 K): δ = 152.7 (1), 152.1, 135.5 (16, 19), 145.0, 140.3 (6, 9), 144.3 (3), 142.2, 137.8 (11. 14), 141.5 (4), 139.1 (C_1–10-Tol), 138.0 (C_1–15-Tol), 137.3 (C_4–21-Tol), 137.1 (C_1–3-Ph), 137.0 (C_4–15-Tol), 136.9 (C_4–10-Tol), 136.8 (C_4–5-Tol), 136.7 (C_1–5-Tol), 136.5, 135.8 (5-*o*-Tol), 136.3 (2), 134.8 (10-*o*-Tol, 15-*o*-Tol), 134.7 (15-*o*-Tol), 134.6 (10-*o*-Tol), 132.8 (2-Ph), 132.2 (3-*o*-Ph), 130.0 (3-*o*-Ph, 13), 129.5 (8, C_1–21-Tol), 128.8 (17), 128.7 (7), 128.4, 127.5 (5-*m*-Tol), 128.3 (15-*m*-Tol), 128.2 (21-*m*-Tol), 128.0 (5, 10-*m*-Tol), 127.9 (10-*m*-Tol), 127.1 (3-*m*-Ph, 12), 127.0 (3-*m*-Ph), 125.6 (3-*p*-Ph), 123.5 (21-*o*-Tol), 118.5 (15), 117.2 (18), 116.3 (10), 88.5 (21), 21.8 (10-*p*-Me), 21.7 (15-*p*-Me), 21.4 (5-*p*-Me), 20.6 ppm (21-*p*-Me); HRMS (ESI): *m*/*z* calcd for $C_{60}H_{44}N_3Ag^+$: 913.2586, found: 913.2393 $[M]^+$; UV/Vis (CH_2Cl_2, 298 K): $\lambda_{max}(\log\varepsilon)$ = 337 (5.45), 368 (5.41), 465 (6.73), 591 nm (5.13 $M^{-1}cm^{-1}$).

Copper(III) carbacorrole (8-Cu): Compound *iso*-**8** (16 mg, 0.02 mmol) was dissolved in freshly distilled tetrahydrofuran (20 mL), then excess $Cu(CH_3COO)_2{\cdot}H_2O$ was added. The mixture was heated to reflux for 1 h. The solvent was removed under reduced pressure. The residue was dissolved in dichloromethane and separated by chromatography on a silica gel (mesh 70–230) column. The first red-green band was collected and evaporated to dryness. The residue contains practically pure **8**-Cu complex. Yield: 16.6 mg (95%), ^{1}H NMR ($CDCl_3$, 230 K): δ = 8.85, 6.30 (2d, 2H; 2-*o*-Ph, 190 K), 8.66 (d, 1H; 7), 8.60 (d, 1H; 18), 8.49 (d, 1H; 13), 8.48 (d, 1H; 8), 8.47 (d, 1H; 17), 8.23 (d, 1H; 12), 8.22 (d, 1H; 15-*o*-Tol), 7.92 (d, 1H; 10-*o*-Tol), 7.88 (d, 2H; 5-*o*-Tol, 10-*o*-Tol), 7.71 (d, 1H; 3-*o*-Ph), 7.69 (d, 1H; 5-*o*-Tol), 7.64 (d, 1H; 15-*o*-Tol), 7.58 (d, 1H; 15-*m*-Tol), 7.50 (d, 1H; 10-*m*-Tol), 7.46 (d, 1H; 10-*m*-Tol), 7.42 (d, 1H; 15-*m*-Tol), 7.34 (t, 1H; 2-*m*-Ph), 7.32 (d, 1H; 5-*m*-Tol), 7.24 (t, 1H; 3-*m*-Ph), 7.18 (t, 1H; 2-*m*-Ph), 7.05 (m, 1H; 3-*p*-Ph), 6.98 (m, 1H; 2-*p*-Ph, 190 K) 6.82 (d, 1H; 5-*m*-Tol), 6.61 (t, 1H; 3-*m*-Ph), 6.00 (d, 1H; 3-*o*-Ph), 5.63 (d, 2H; 21-*m*-Tol), 4.21 (d, 2H; 21-*o*-Tol), 2.59 (s, 3H; 10-*p*-Me), 2.58 (s, 3H; 15-*p*-Me), 2.37 (s, 3H; 5-*p*-Me), 1.36 ppm (s, 3H; 21-*p*-Me); ^{13}C NMR ($CDCl_3$, 230 K): δ = 149.6 (1), 148.7, 142.2 (6, 9), 146.1, 138.2 (16, 19), 144.6, 141.0 (11, 14), 143.7 (3), 141.0 (C_1–2-Ph), 139.6 (4), 138.5 (C_1–10-Tol), 138.4 (C_4–21-Tol), 137.5 (C_4–10-Tol), 137.4 (C_4–5-Tol), 137.3 (C_4–15-Tol), 137.2 (C_1–3-Ph), 137.0 (C_1–15-Tol), 136.5 (2), 136.3 (C_1–5-Tol), 135.1 (5-*o*-Tol), 134.2, 134.0 (15-*o*-Tol), 134.1 (10-*o*-Tol), 133.9, 133.8 (5-*o*-Tol, 10-*o*-Tol), 132.8, 129.5 (3-*o*-Ph), 132.3 (2-*o*-Ph), 130.7 (5), 130.5 (C_1–21-Tol), 130.4 (13), 129.8 (8), 129.0, 125.9 (2-*m*-Ph), 128.6 (17),

128.46, 128.48 (15-*m*-Tol), 128.3 (21-*m*-Tol), 128.1 (5-*m*-Tol, 10-*m*-Tol), 128.0 (5-*m*-Tol, 10-*m*-Tol, 7), 127.5 (2-*p*-Ph), 127.4 (12), 127.2, 127.0 (3-*m*-Ph), 125.6 (3-*p*-Ph), 121.0 (21-*o*-Tol), 120,1 (10), 118.9 (15, 18), 96.4 (21), 21.41 (15-*p*-Me), 21.37 (10-*p*-Me), 21.2 (5-*p*-Me), 20.3 ppm (21-*p*-Me); HRMS (ESI): *m*/*z* calcd for $C_{60}H_{44}N_3Cu^+$: 869.2831, found: 869.2742 $[M]^+$; UV/Vis (CH_2Cl_2, 298 K): λ_{max} ($\log\varepsilon$) = 417 (5.57), 452 (5.71) 585 (5.15) 605 nm (5.14 $M^{-1}cm^{-1}$).

21-Oxacorrole (9): Compound **8**-Ag (0.02 mmol, 16 mg) was dissolved in dichloromethane (20 mL), then water (2 mL) and hydrochloric acid (2 mL, 38% in H_2O) was added. The mixture was stirred for 48 h at room temperature. The heterogeneous mixture was poured into water (50 mL), and the organic products were separated. Excess TEA was added, and the mixture was evaporated to dryness. The residue was dissolved in dichloromethane/hexane (5:5 v/v) and separated by chromatography on a basic alumina (grade II) column. The first pink fraction was collected and evaporated to afford **9** (6.3 mg, 50%). ^{1}H NMR ($CDCl_3$, 298 K): δ = 8.89 (d, 1H; 18), 8.85 (d, 1H; 13), 8.72 (d, 1H; 7), 8.68 (d, 1H; 17), 8.67 (d, 1H; 8), 8.61(d, 1H; 12), 8.15 (d, 2H; 15-*o*-Tol), 8.06 (d, 2H; 10-*o*-Tol), 8.00 (d, 2H; 2-*o*-Ph), 7.65 (d, 2H; 5-*o*-Tol), 7.61 (t, 2H; 2-*m*-Ph), 7.57 (d, 2H; 15-*m*-Tol), 7.56 (t, 1H; 2-*p*-Ph), 7.52 (d, 2H; 10-*m*-Tol), 7.20 (d, 2H; 3-*o*-Ph), 7.16 (t, 1H; 3-*p*-Ph), 7.07 (t, 2H; 3-*m*-Ph), 7.02 (d, 2H; 5-*m*-Tol), 2.66 (s, 3H; 10-*p*-Me), 2.65 (s, 3H; 15-*p*-Me), 2.41 (s, 3H; 5-*p*-Me), −2.86 ppm (s, 1H; 22-NH); ^{13}C NMR ($CDCl_3$, 298 K): δ = 152.4, 150.4 (11, 14), 143.5, 136.2 (1, 4), 139.6 (C_1–10-Tol), 137.8 (C_1–15-Tol), 137.5, 135.7 (6, 9), 137.5 (C_4–15-Tol), 137.2 (C_4–5-Tol), 137.0 (C_4–10-Tol), 135.0 (15-*o*-Tol), 134.8 (10-*o*-Tol), 134.7 (5-*o*-Tol), 134.5, 123.8 (16, 19), 134.3 (C_1–5-Tol), 134.2 (C_1–3-Ph), 133.7 (C_1–2-Ph), 132.2 (2-*o*-Ph), 132.0 (3, 3-*o*-Ph), 131.7 (13), 130.4 (12), 129.5 (2), 128.8 (15-*m*-Tol), 128.6 (2-*m*-Ph), 128.3 (2-*p*-Ph), 127.9 (10-*m*-Tol), 127.8 (5-*m*-Tol), 127.5 (3-*m*-Ph), 126.0 (7, 3-*p*-Ph), 125.9 (8), 123.1 (17), 120.0 (15), 116.0 (18), 113.8 (10), 108.1 (5), 21.70 (15-*p*-Me), 21.66 (10-*p*-Me), 21.4 ppm (5-*p*-Me); HRMS (ESI): *m*/*z* calcd for $C_{52}H_{40}N_3O^+$: 722.3166, found: 722.3173 $[M+H]^+$; UV/Vis (CH_2Cl_2, 298 K): λ_{max}($\log\varepsilon$) = 410 (5.70), 426 (5.50), 493 (4.18), 526 (4.52), 562 (4.97), 614 nm (4.68 $M^{-1}cm^{-1}$).

Acknowledgements

Financial support from the Ministry of Science and Higher Education (Grant PBZ-KBN-118/T09/2004) is kindly acknowledged. Quantum chemical calculations were carried out at the Poznañ Supercomputer Center (Poznañ) and Wrocław Supercomputer Center (Wrocław).

[1] J. L. Sessler, D. Seidel, *Angew. Chem.* **2003**, *115*, 5292–5333; *Angew. Chem. Int. Ed.* **2003**, *42*, 5134–5175.
[2] J. L. Sessler, S. J. Weghorn, *Expanded, Contracted, and Isomeric Porphyrins*, Elsevier Science, **1997**.
[3] H. Furuta, H. Maeda, A. Osuka, *Chem. Commun.* **2002**, 1795–1804.
[4] M. Pawlicki, L. Latos-Grażyński, *Chem. Rec.* **2006**, *6*, 64–78.
[5] L. Latos-Grażyński, in *The Porphyrin Handbook, Vol. 2*, (Eds.: K. M. Kadish, K. M. Smith, R. Guilard), Academic Press, New York **2000**, pp. 361–416.
[6] I. Gupta, M. Ravikanth, *Coord. Chem. Rev.* **2006**, *250*, 468–518.
[7] P. J. Chmielewski, L. Latos-Grażyński, *Coord. Chem. Rev.* **2005**, *249*, 2510–2533.
[8] L. Latos-Grażyński, E. Pacholska, P. J. Chmielewski, M. M. Olmstead, A. L. Balch, *Angew. Chem.* **1995**, *107*, 2467–2469; *Angew. Chem. Int. Ed. Engl.* **1995**, *34*, 2252–2254.
[9] M. Abe, M. R. Detty, O. O. Gerlits, D. K. Sukumaran, *Organometallics* **2004**, *23*, 4513–4518.
[10] E. Pacholska, L. Latos-Grażyński, Z. Ciunik, *Chem. Eur. J.* **2002**, *8*, 5403–5406.
[11] E. Pacholska, L. Latos-Grażyński, Z. Ciunik, *Angew. Chem.* **2001**, *113*, 4598–4601; *Angew. Chem. Int. Ed.* **2001**, *40*, 4466–4469.
[12] P. J. Chmielewski, L. Latos-Grażyński, K. Rachlewicz, T. Głowiak, *Angew. Chem.* **1994**, *106*, 805–808; *Angew. Chem. Int. Ed. Engl.* **1994**, *33*, 779–781.
[13] H. Furuta, T. Asano, T. Ogawa, *J. Am. Chem. Soc.* **1994**, *116*, 767–768.
[14] L. Szterenberg, N. Sprutta, L. Latos-Grażyński, *J. Inclusion Phenom. Macrocyclic Chem.* **2001**, *41*, 209–213.
[15] N. Sprutta, L. Latos-Grażyński, *Tetrahedron Lett.* **1999**, *40*, 8457–8460.
[16] M. J. Chmielewski, M. Pawlicki, N. Sprutta, L. Szterenberg, L. Latos-Grażyński, *Inorg. Chem.* **2006**, *45*, 8664–8671.
[17] M. Pawlicki, L. Latos-Grażyński, *J. Org. Chem.* **2005**, *70*, 9123–9130.
[18] M. Pawlicki, L. Latos-Grażyński, L. Szterenberg, *Inorg. Chem.* **2005**, *44*, 9779–9786.
[19] M. Pawlicki, L. Latos-Grażyński, *Chem. Eur. J.* **2003**, *9*, 4650–4660.
[20] N. Sprutta, L. Latos-Grażyński, *Org. Lett.* **2001**, *3*, 1933–1936.
[21] E. Pacholska, L. Latos-Grażyński, L. Szterenberg, Z. Ciunik, *J. Org. Chem.* **2000**, *65*, 8188–8196.
[22] A. Ulman, J. Manassen, *J. Chem. Soc. Perkin Trans. 1* **1979**, 1066–1069.
[23] A. Ulman, J. Manassen, F. Frolow, D. Rabinowich, *Tetrahedron Lett.* **1978**, *19*, 1885–1886.
[24] A. Ulman, J. Manassen, F. Frolow, D. Rabinowich, *Tetrahedron Lett.* **1978**, *19*, 167–170.
[25] A. Ulman, J. Manassen, *J. Am. Chem. Soc.* **1975**, *97*, 6540–6544.
[26] P. J. Chmielewski, L. Latos-Grażyński, M. M. Olmstead, A. L. Balch, *Chem. Eur. J.* **1997**, *3*, 268–278.
[27] L. Latos-Grażyński, J. Lisowski, M. M. Olmstead, A. L. Balch, *J. Am. Chem. Soc.* **1987**, *109*, 4428–4429.
[28] L. Latos-Grażyński, E. Pacholska, P. J. Chmielewski, M. M. Olmstead, A. L. Balch, *Inorg. Chem.* **1996**, *35*, 566–573.
[29] Y. Matano, T. Nakabuchi, T. Miyajima , H. Imahori, H. Nakano, *Org. Lett.* **2006**, *8*, 5713–5716.
[30] Y. Matano, T. Nakabuchi, T. Miyajima , H. Imahori, *Organometallics* **2006**, *25*, 3105–3107.
[31] Y. Matano, T. Miyajima, T. Nakabuchi , H. Imahori, N. Ochi, S. Sakaki, *J. Am. Chem. Soc.* **2006**, *128*, 11760–11761.
[32] K. Tamao, S. Yamaguch, M. Shiro, *J. Am. Chem. Soc.* **1994**, *116*, 11715–11722.
[33] S. Yamaguchi, T. Endo, M. Uchida, T. Izumizawa, K. Furukawa, K. Tamao, *Chem. Eur. J.* **2000**, *6*, 1683–1692.
[34] S. Yamaguchi, K. Tamao, *J. Organomet. Chem.* **2002**, *653*, 223–228.
[35] J.-H. Fuhrhop, D. Mauzerall, *J. Am. Chem. Soc.* **1968**, *90*, 3875–3876.
[36] B. Krattinger, H. J. Callot, *Tetrahedron Lett.* **1996**, *37*, 7699–7702.
[37] B. Krattinger, H. J. Callot, *Tetrahedron Lett.* **1998**, *39*, 1165–1168.
[38] R. Ruppert, C. Jeandon, A. Sgambati, H. J. Callot, *Chem. Commun.* **1999**, 2123–2124.
[39] B. Krattinger, H. J. Callot, *Eur. J. Org. Chem.* **1999**, 1857–1867.
[40] J.-W. Ka, C.-H. Lee, *Tetrahedron Lett.* **2001**, *42*, 4527–4529.
[41] R. Myśliborski, L. Latos-Grażyński, *Eur. J. Org. Chem.* **2005**, 5039–5048.
[42] M. Stępień, L. Latos-Grażyński, *Chem. Eur. J.* **2001**, *7*, 5113–5117.
[43] C. Nervi, R. Gobetto, L. Milone, A. Viale, E. Rosenberg, D. Rokhsana, J. Fiedler, *Chem. Eur. J.* **2003**, *9*, 5749–5756.
[44] R. W. Kreilick in *NMR of Paramagnetic Molecules. Principles and Applications* (Eds.: G. N. La Mar, W. D. Horrocks, Jr., R. H. Holm), Academic Press, New York **1973**, pp. 595–626.
[45] T. J. Swift in *NMR of Paramagnetic Molecules. Principles and Applications* (Eds.: G. N. La Mar, W. D. Horrocks, Jr., R. H. Holm), Academic Press, New York **1973**, pp. 53–83.
[46] I. Bertini, C. Luchinat, *Coord. Chem. Rev.* **1996**, *150*, 1–296.
[47] Z. Duan , M. Clochard, B. Donnadieu, F. Mathey, F. S. Tham, *Organometallics* **2007**, *26*, 3617–3620.
[48] Y. Hirata, H. Furuta, A. Srinivasan, *Nippon Kagakkai Koen Yokoshu* **2005**, *85*, 1418–1418.

[49] C. Jeandon, R. Ruppert, H. J. Callot, *Chem. Commun.* **2004**, 1090–1091.
[50] M. Senge, N. N. Segeeva, *Angew. Chem.* **2006**, *118*, 7654–7657; *Angew. Chem. Int. Ed.* **2006**, *45*, 7492–7495.
[51] C. Jeandon, R. Ruppert, H. J. Callot, *J. Org. Chem.* **2006**, *71*, 3111–3120.
[52] D. Sanz , M. Peréz-Torralba, S. H. Alarcón, R. M. Claramunt, C. Foces-Foces, J. Elguero, *J. Org. Chem.* **2002**, *67*, 1462–1471.
[53] R. Balasubramanian, M. V. George, *J. Organomet. Chem.* **1975**, *85*, 311–316.
[54] J. Chen , B. Xiu, X. Ouyang, B. Z. Tang, Y. Cao, *J. Phys. Chem. A* **2004**, *108*, 7522–7526.
[55] M. D. Curtis, *J. Am. Chem. Soc.* **1969**, *91*, 6011–6018.
[56] S. Yamaguchi, T. Endo, M. Uchida, T. Izumizawa, K. Furukawa, K. Tamao, *Chem. Eur. J.* **2000**, *6*, 1683–1692.
[57] J. Ohshita, N. Honda, K. Nada, T. Iida, T. Mihara, Y. Matsuo, A. Kunai, A. Naka, M. Ishikawa, *Organometallics* **2003**, *22*, 2436–2441.
[58] A. Kunai, T. Mihara, Y. Matsuo, J. Ohshita, A. Naka, M. Ishikawa, *J. Organomet. Chem.* **1997**, *546*, 611–613.
[59] M. Takahashi, S. Tsutsui, K. Sakamato, M. Kira, T. Muller, Y. Apeloig, *J. Am. Chem. Soc.* **2001**, *123*, 347–348.
[60] S. Tsutsui, K. Sakamoto, M. Kira, *J. Am. Chem. Soc.* **1998**, *120*, 9955–9956.
[61] H. Ubayama, W.-H. Sun, Z. Xi, T. Takahashi, *Chem. Commun.* **1998**, 1931–1932.
[62] J. S. Drage, P. C. Vollhardt, *Organometallics* **1985**, *4*, 389–398.
[63] L. F. Veiros, G. Dazinger, K. Kirchner, M. J. Calhorda, R. Schmid, *Chem. Eur. J.* **2004**, *10*, 5860–5870.
[64] Y. Liu, M. Liu, Z. Song, *J. Am. Chem. Soc.* **2005**, *127*, 3662–3663.
[65] S. Zhou , B. Yan, Y. Liu, *J. Org. Chem.* **2005**, *70*, 4006–4012.
[66] C.-H. Lee, W.-S. Cho, J.-W. Ka, H.-J. Kim, P. H. Lee, *Bull. Korean Chem. Soc.* **2000**, *21*, 429–433.
[67] H. Furuta, T. Ogawa, Y. Uwatoko, K. Araki, *Inorg. Chem.* **1999**, *38*, 2676–2682.
[68] M. A. Muckey, L. F. Szczepura, G. M. Ferrence, T. D. Lash, *Inorg. Chem.* **2002**, *41*, 4840–4842.
[69] H. Furuta, H. Maeda, A. Osuka, *J. Am. Chem. Soc.* **2000**, *122*, 803–807.
[70] A. Ghosh, in *The Porphyrin Handbook, Vol. 7*, (Eds.: K. M. Kadish, K. M. Smith, R. Guilard), Academic Press, San Diego, CA **2000**, pp. 1–38.
[71] M. Stępień, L. Latos-Grażyński, T. D. Lash, L. Szterenberg, *Inorg. Chem.* **2001**, *40*, 6892–6900.
[72] M. Stępień, L. Latos-Grażyński, L. Szterenberg, *J. Org. Chem.* **2007**, *72*, 2259–2270.
[73] R. Myśliborski, L. Latos-Grażyński, L. Szterenberg, T. Lis, *Angew. Chem.* **2006**, *118*, 3752–3756; *Angew. Chem. Int. Ed.* **2006**, *45*, 3670–3674.
[74] M. Stępień, L. Latos-Grażyński, L. Szterenberg, *Inorg. Chem.* **2004**, *43*, 6654–6662.
[75] M. Stępień, L. Latos-Grażyński, L. Szterenberg, J. Panek, Z. Latajka, *J. Am. Chem. Soc.* **2004**, *126*, 4566–4580.
[76] M. Pawlicki, L. Latos-Grażyński, L. Szterenberg, *J. Org. Chem.* **2002**, *67*, 5644–5653.
[77] L. Szterenberg, L. Latos-Grażyński, *Inorg. Chem.* **1997**, *36*, 6287–6291.
[78] M. J. Bain-Ackerman, D. K. Lavallee, *Inorg. Chem.* **1979**, *18*, 3358–3364.
[79] P. Hambright, P. B. Chock, *J. Am. Chem. Soc.* **1974**, *96*, 3123–3131.
[80] R. F. Longo, E. M. Brown, D. J. Quimby , A. D. Adler, M. Meot-Ner, *Ann. N. Y. Acad. Sci.* **1973**, *206*, 420–442.
[81] R. F. Longo, E. M. Brown, G. W. Rau, A. D. Adler in *The Porphyrins ,Vol. 5*, (Ed.: D. Dolphin), Academic Press, New York **1978**, pp. 459–481.
[82] Sheldrick, G. M. SHELXS 97 - Program for Crystal Structure Solution. **1997**. University of Göttingen.
[83] Sheldrick, G. M. SHELXL 97 - Program for Crystal Structure Refinement, **1997**, University of Göttingen.
[84] Gaussian 03, Revision C.02, M. J. Frisch, G. W. Trucks, H. B. Schlegel, G. E. Scuseria, M. A. Robb, J. R. Cheeseman, J. A. Montgomery, Jr., T. Vreven, K. N. Kudin, J. C. Burant, J. M. Millam, S. S. Iyengar, J. Tomasi, V. Barone, B. Mennucci, M. Cossi, G. Scalmani, N. Rega, G. A. Petersson, H. Nakatsuji, M. Hada, M. Ehara, K. Toyota, R. Fukuda, J. Hasegawa, M. Ishida, T. Nakajima, Y. Honda, O. Kitao, H. Nakai, M. Klene, X. Li, J. E. Knox, H. P. Hratchian, J. B. Cross, V. Bakken, C. Adamo, J. Jaramillo, R. Gomperts, R. E. Stratmann, O. Yazyev, A. J. Austin, R. Cammi, C. Pomelli, J. W. Ochterski, P. Y. Ayala, K. Morokuma, G. A. Voth, P. Salvador, J. J. Dannenberg, V. G. Zakrzewski, S. Dapprich, A. D. Daniels, M. C. Strain, O. Farkas, D. K. Malick, A. D. Rabuck, K. Raghavachari, J. B. Foresman, J. V. Ortiz, Q. Cui, A. G. Baboul, S. Clifford, J. Cioslowski, B. B. Stefanov, G. Liu, A. Liashenko, P. Piskorz, I. Komaromi, R. L. Martin, D. J. Fox, T. Keith, M. A. Al-Laham, C. Y. Peng, A. Nanayakkara, M. Challacombe, P. M. W. Gill, B. Johnson, W. Chen, M. W. Wong, C. Gonzalez, J. A. Pople, **2004**, Wallingford CT, Gaussian Inc.
[85] A. D. Becke, *Phys. Rev. A* **1988**, *38*, 3098–3100.
[86] C. Lee, W. Yang, R. G. Parr, *Phys. Rev. B* **1988**, *37*, 785–789.

Received: December 19, 2007
Published online: April 9, 2008

